

Journal Pre-proof

Stacked Hybridization to Enhance the Performance of Artificial Neural Networks (ANN) for Prediction of Water Quality Index in the Bagh River Basin, India

Nand Lal Kushwaha, Nanabhau S. Kudnar, Dinesh Kumar Vishwakarma, A. Subeesh, Malkhan Singh Jatav, Venkatesh Gaddikeri, Ashraf A. Ahmed, Ismail Abdelaty

PII: S2405-8440(24)07116-0

DOI: <https://doi.org/10.1016/j.heliyon.2024.e31085>

Reference: HLY 31085

To appear in: *HELIYON*

Received Date: 7 February 2024

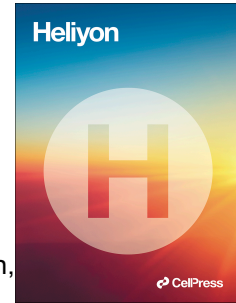
Revised Date: 3 May 2024

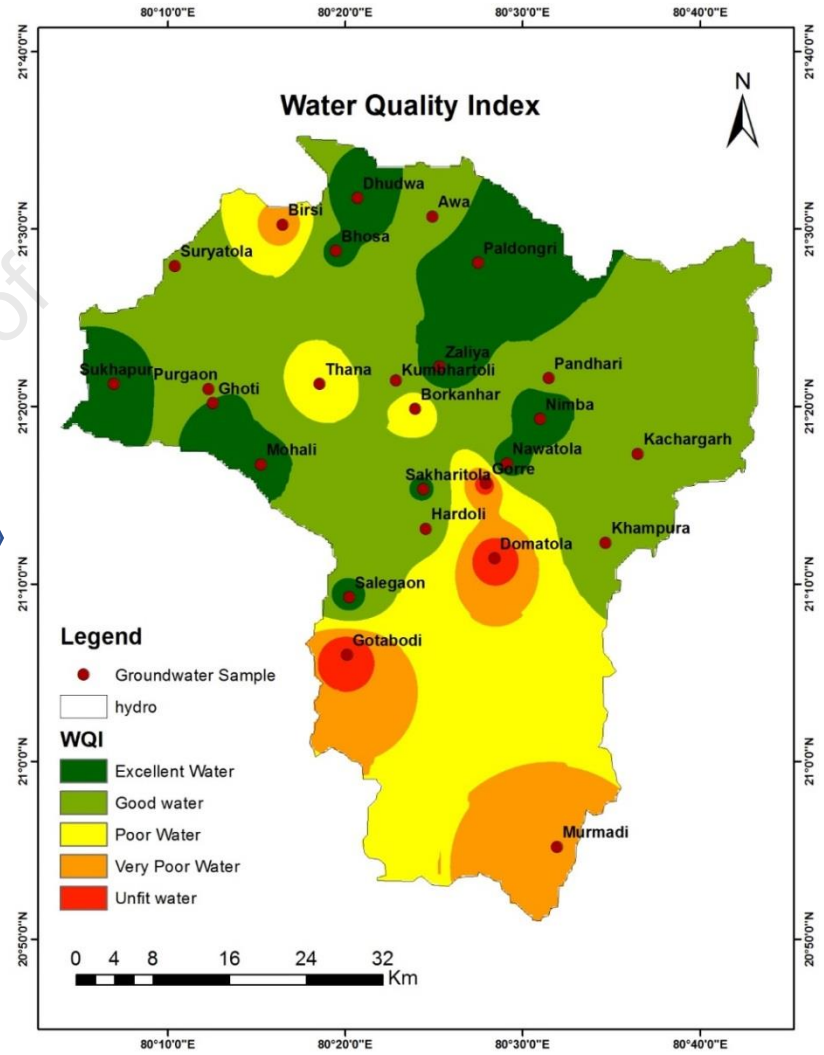
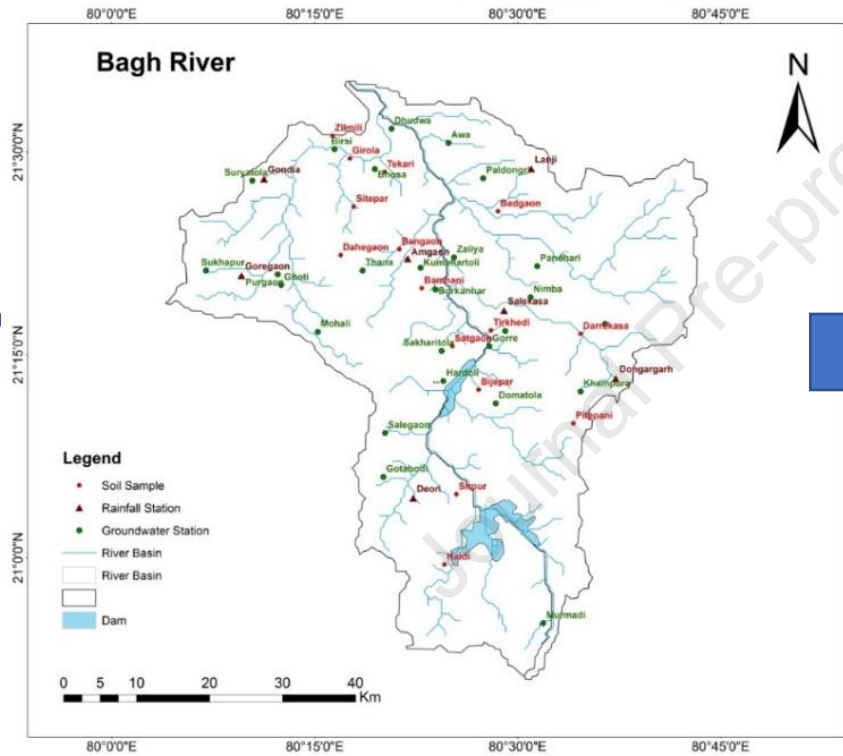
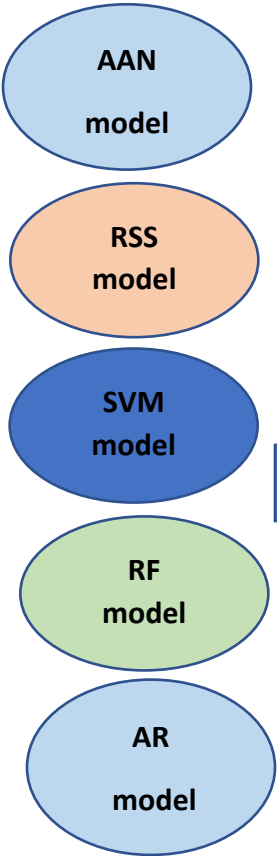
Accepted Date: 9 May 2024

Please cite this article as: Stacked Hybridization to Enhance the Performance of Artificial Neural Networks (ANN) for Prediction of Water Quality Index in the Bagh River Basin, India, *HELIYON*, <https://doi.org/10.1016/j.heliyon.2024.e31085>.

This is a PDF file of an article that has undergone enhancements after acceptance, such as the addition of a cover page and metadata, and formatting for readability, but it is not yet the definitive version of record. This version will undergo additional copyediting, typesetting and review before it is published in its final form, but we are providing this version to give early visibility of the article. Please note that, during the production process, errors may be discovered which could affect the content, and all legal disclaimers that apply to the journal pertain.

© 2024 Published by Elsevier Ltd.





Data Acquisition for Bagh River Basin, India and Spatial distribution of WQI

Stacked Hybridization to Enhance the Performance of Artificial Neural Networks (ANN) for Prediction of Water Quality Index in the Bagh River Basin, India

Nand Lal Kushwaha^{a,b}, Nanabhau S. Kudnar^c, Dinesh Kumar Vishwakarma^d, A Subeesh^e, Malkhan Singh Jatav^f, Venkatesh Gaddikeri^b, Ashraf A Ahmed^{g,*} and Ismail Abdelaty^h

^aDepartment of Soil and Water Engineering, Punjab Agricultural University Ludhiana, Punjab, 141004, India, Email: nand.kushwaha@icar.gov.in (N.L. Kushwaha)

^bDivision of Agricultural Engineering, ICAR-Indian Agricultural Research Institute, New Delhi, 110012, India, venkatg303@gmail.com (Venkatesh Gaddikeri)

^cDepartment of Geography, C. J. Patel College Tirora, Gondia, Maharashtra, 441911, India, Email: nanabhaukudnar@gmail.com

^dDepartment of Irrigation and Drainage Engineering, G.B. Pant University of Agriculture and Technology, Pantnagar, Uttarakhand, 263145, India, Email: dinesh.vishwakarma4820@gmail.com

^eICAR- Central Institute of Agricultural Engineering, Bhopal, Madhya Pradesh, 462038, India, Email: subeesh18@gmail.com

^fNational Institute of Hydrology, North Western Regional Centre, Jodhpur, Rajasthan, 342003, India, Email: msjatav1168@gmail.com

^gDepartment of Civil and Environmental Engineering, Brunel University London, Kingston Lane, Uxbridge UB38PH, UK, Email: ashraf.ahmed@brunel.ac.uk

^hWater and Water Structures Engineering Department, Faculty of Engineering, Zagazig University, Zagazig, 44519, Egypt, Email: Eng_abdelaty2006@yahoo.com

*Corresponding author's email: ashraf.ahmed@brunel.ac.uk

Abstract

Water quality assessment is paramount for environmental monitoring and resource management, particularly in regions experiencing rapid urbanization and industrialization. This study introduces Artificial Neural Networks (ANN) and its hybrid machine learning models, namely ANN-RF (Random Forest), ANN-SVM (Support Vector Machine), ANN-RSS (Random Subspace), ANN-M5P (M5 Pruned), and ANN-AR (Additive Regression) for water quality assessment in the rapidly urbanizing and industrializing Bagh River Basin, India. The Relief algorithm was employed to select the most influential water quality input parameters, including Nitrate (NO_3^-), Magnesium (Mg^{2+}), Sulphate (SO_4^{2-}), Calcium (Ca^{2+}), and Potassium (K^+). The comparative analysis of developed ANN and its hybrid models was carried out using statistical indicators (i.e., Nash-Sutcliffe Efficiency (NSE), Pearson Correlation Coefficient (PCC), Coefficient of Determination (R^2), Mean Absolute Error (MAE), Root Mean Square Error (RMSE), Relative Root Square Error (RRSE), Relative Absolute Error (RAE), and Mean Bias Error (MBE) and graphical representations (i.e., Taylor diagram). Results indicate that the integration of support vector machine (SVM) with ANN significantly improves performance, yielding impressive statistical indicators: NSE (0.879), R^2 (0.904), MAE (22.349), and MBE (12.548). The methodology outlined in this study can serve as a template for enhancing the predictive capabilities of ANN models in various other environmental and ecological applications, contributing to sustainable development and safeguarding natural resources.

44 **Keywords:** Groundwater, Water quality assessment, SVM, Water resources management,
45 Machine learning

46 1. Introduction

47 Assessing and forecasting water quality holds significant importance in the realm of
48 integrated water resource management. This domain recognizes groundwater as vital for
49 human well-being and future progress [1]. The fundamental problem of managing water
50 resources in stressful areas, particularly in developing nations [2,3]. Due to the release of
51 contamination and its impact on the value of water properties globally, river basin water
52 quality is an issue. The key to implementing methods for managing water resources in river
53 basins and addressing the issue of river water pollution is to reduce river basin pollution by
54 identifying the drivers and water quality metrics [4,5]. Since the industrial revolution, one of
55 humanity's significant pertinent trials is the river water quality, which has been at high risk
56 and deteriorating [6]. Predictive models are useful for evaluating the influence of hydrological
57 and anthropogenic water stress on water value variables [7]. The lack of a shared blueprint
58 for water quality data is a problem for most hydrological flux concentration databases, which
59 produce relatively high time resolution [8]. In arid and semi-arid areas, water supplies are
60 scarce while industry demands, drinking water, and agriculture are rising, particularly in areas
61 experiencing drought [9,10].

62 Machine Learning (ML) models are effective methods for minimizing source
63 quantification mistakes that cannot be avoided [11]. Additionally, the poorly understood
64 biogeochemical and physical processes that drive the transport and transformation of
65 pollutants are subject to fewer parameterization limits in the ML models. Machine learning is
66 created to identify nonlinear behavior [12]. Artificial intelligence (AI) approaches are used
67 more often in various fields. It is employed in hydrological forecasting and produces highly
68 accurate river flow predictions [13]. Artificial intelligence is a good alternative and
69 complements conventional methods for investigation and prediction. Using physical
70 characteristics in groundwater resources irrigation water quality indexes (IWQI) is expensive
71 and time-consuming for farmers, especially in developing nations [14]. Machine learning
72 models are highly effective in reducing source quantification errors that cannot be eliminated
73 by any other means [15].

74 To measure and assess the overall water quality index (WQI), Horton [16] suggested
75 combining various factors into a single number. To estimate the suitability of groundwater for
76 irrigation reasons using 13 physicochemical characteristics, Wagh et al. [17] utilized the
77 artificial neural networks (ANN) model; the study revealed that ML models are quite accurate
78 in predicting and examining water quality. Another study [18] in southeastern Nigeria
79 leverages machine learning to enhance water quality analysis, a relatively unexplored area in
80 the country. Employing integrated algorithms, the research accurately models groundwater
81 quality, revealing 80% of the resources as potable. Cluster analyses pinpoint contamination
82 sources and spatial variations. Notably, both multiple linear regression and neural networks
83 yield precise water quality predictions, underscoring their potential for advancing sustainable
84 water management practices. Using k-means clustering in the major European rivers, Massei
85 et al. [19] evaluated the impact of pesticides and biocides in river water on hazardous risk. To
86 enhance the performances of individual models for the salinity and chlorophyll in beach
87 water, particularly for multi-step ahead modeling, Shamshirband et al. [20] used multiple
88 wavelets-ANNs models. Another study by Di et al. [21] developed classification ML models for
89 IWQ prediction in the Yangtze River. Similarly, Ahmed et al. [22] provided a thorough review
90 of different machine learning models used for water quality .

91 Water quality research has made significant progress in recent times, the use of various
92 modeling approaches that have been applied to tackle different aspects of the issue. Castrillo
93 and García (2020) utilized random forest (RF) and linear models to tackle high-nutrient levels
94 in the river Thames. Meanwhile, Bui et al. [23] delved into WQI forecasting, exploring a
95 combination of 4 conventional methods and 12 hybrid AI strategies. Their study showed that
96 hybrid AI models outperformed conventional ones regarding predictive accuracy. Nafi et al.
97 [24] introduced RF and random tree (RT) methods for classifying river water quality,
98 considering parameters like thermal conductivity, temperature, total and fecal coliform
99 concentrations, demand for biological oxygen, and nitrate. Agbasi and Egbueri [25]
100 investigated water pollution in Umunya, Nigeria, using various indices like Human Health Risk
101 (HHRISK), Modified heavy metal index (MHMI), Synthetic pollution index (SPI), and Entropy-
102 weighted water quality index (EWQI),. Results show that 60% of samples are safe for
103 consumption, but 40% pose risks, especially to children. Carcinogenic risks are high, and
104 ingestion poses a greater risk than dermal contact. Artificial neural networks and multiple
105 linear regression models provided precise predictions of water quality indices, while

106 hierarchical dendrograms effectively categorized the water samples into different
107 spatiotemporal water quality clusters. Jahin et al. [26] opted for multivariate analysis to study
108 the IWQI for surface water in Egypt. Elbeltagi et al. [27] took a different approach by
109 evaluating WQI at the Akot basin. They employed Support Vector Machine (SVM), random
110 subspace (RSS), and additive regression (AR). Notably, the AR model was recommended due
111 to its simplicity in terms of input parameters while maintaining reliability and accurate
112 prediction.

113 In another study, Kouadri et al. [28] used a machine learning model to predict the water
114 quality index (WQI) in Illizi, Southeast Algeria, particularly focusing on irregular data. They
115 identified total dissolved solids (TDS) and total hardness (TH) as the main factors influencing
116 WQI, with the mean absolute error (MAE) model proving to be the most accurate among the
117 methods considered. Valentini et al. [29] developed a new WQI equation for Mirim Lagoon
118 based on extensive data collected over three years at seven locations, with parameters
119 including pH, dissolved oxygen, conductivity, turbidity, fecal coliform, and temperature. The
120 study [30] in Pratapgarh, Southern Rajasthan, employs an artificial neural network (ANN) to
121 predict groundwater sodium hazards for irrigation. Using MATLAB and ten years of data, the
122 optimized ANN model effectively forecasts water quality indicators like sodium adsorption
123 ratio (SAR), percent sodium (%Na) residual, Kelly's ratio (KR), and residual sodium carbonate
124 (RSC). Finally, Shukla et al. [31] conducted a comparative analysis, evaluating a feed-forward
125 artificial neural network (ANN) model against other algorithms. Their findings suggested that
126 a more complex architecture involving the integration of the ANN algorithm with wavelets or
127 an adaptive neuro-fuzzy reasoning system yielded superior results, particularly in accurately
128 predicting stream flow in an Indian river.

129 Previous works indicated limited research focusing on developing hybrid machine learning
130 models specifically tailored for predicting water quality, especially within the context of Indian
131 conditions. In response to this gap, the present study delves into assessing the performance
132 of various models, including Artificial Neural Networks (ANN) and its hybrid combinations,
133 namely ANN-RF (Random Forest), ANN-SVM (Support Vector Machine), ANN-RSS (Random
134 Subspace), ANN-M5P (M5 Pruned), and ANN-AR (Additive Regression). These models were
135 applied to evaluate the Water Quality Index (WQI) in the Bagh River Basin, India. The primary
136 objective of this study was not only to assess the performance of the ANN algorithms but also
137 to enhance their predictive capabilities through hybridization with other machine learning

138 algorithms. By doing so, we aimed to identify the most effective and suitable AI-based model
139 for WQI prediction within the specific environmental conditions of the Bagh River Basin. It's
140 crucial to note that the volume and organization of available data play a pivotal role in
141 determining the effectiveness of various machine learning algorithms. Therefore, the selected
142 algorithm ANN and its hybrids were chosen based on their proven track record of delivering
143 robust performance and their aptitude for capturing dynamic, nonlinear relationships within
144 datasets.

145 **2. Methodology**

146 **2.1. Study area and available datasets**

147 The Bagh River is a significant tributary of the Wainganga River [32]. The river basin lies
148 between latitude $20^{\circ} 45' 0''$ N to $21^{\circ} 45' 0''$ N latitude and longitude $80^{\circ} 00' 0''$ E to $80^{\circ} 45' 0''$
149 E (Fig. 1). This river's axial and longitudinal extensions result in a total coverage area of 2876.9
150 Km². This 130 km long river begins in the Cheezgad hills of the Sahyadri mountain range.
151 Given the topography of this river, BRB is situated between the Wainganga River valley to the
152 north, the Gaikhori hills to the west, the valleys to the east, and the Chichgad hills to the
153 south. This river bed has an average elevation between 208 and 728 meters. Two rivers, the
154 Ghisari and Dev Rivers, on its right bank and the Pangoli river on its left, join this river. At
155 Birsola in the Gondia District, the Bagh River merges with the Wainganga River.

156 Because metamorphic and igneous rocks cover the whole river basin, this research
157 region is unlike any other in Maharashtra. The Pre-Cambrian Archaean Dharwars crystalline
158 rocks make up a large portion, the Amgaon Group, which is limited to the northeast and
159 northwest corners of the area surrounding Amgaon and Bahela, is the representative
160 formation of the Archeans [33]. It is made up of Augen gneisses, amphibolites, and
161 migmatites. The Sakoli Group and Dongargarh Group of rocks, which together comprise the
162 main stratigraphic block, is representative of the Lower Precambrian Dharwars, which come
163 after the Amgaon group. The Sakoli Group is limited to the northern and western regions of
164 Nagjhira and is made up of quartzites, schists, phyllites, metavolcanics, and BIF. Rhyolites,
165 Andesites, and basic volcanics are found in the vicinity of Salekasa, Wadegaon, Murdoli, Deori,
166 and Chinchgarh. These rocks correspond to the Dongargarh Group's Bijli, Pitepani, and
167 Sitagota formations [33,34].

168 Groundwater samples were taken from 26 wells in the Bagh River basin during the pre-
169 monsoon season, and analyses were done for the different perimeters. Composite sampling
170 is carried out when the liquid matrix is expected to be heterogeneous and varies from time
171 to time or depth or at many sampling locations. This type of sampling provides a
172 representative sampling for this type of matrix and is carried out by combining portions of
173 multiple grab samples collected at regular intervals. If the flow is expected to be constant,
174 then volume-based sampling can be carried out. If the flow varies, like sewerage line, then
175 sampling can be done by flow-based composite, i.e., collecting sample that is proportional to
176 the discharge. Time composite sampling represents a 24- hour period, with interval being 1-
177 3 hours. Use composite samples only for parameters that will remain unchanged under the
178 sampling conditions, preservation and storage. The factors listed here consist of pH, Sodium
179 (Na^+), Sulfate (SO_4^{2-}), Bicarbonate (HCO_3^-), Total dissolved solids (TDS), Total Hardness (TH),
180 Magnesium (Mg^{2+}), Chloride (Cl^-), Calcium (Ca^{2+}), Nitrate (NO_3^-), and Fluoride (F^-). Collection,
181 preservation, transportation, storage, and weighted arithmetic index method analysis of the
182 sample.

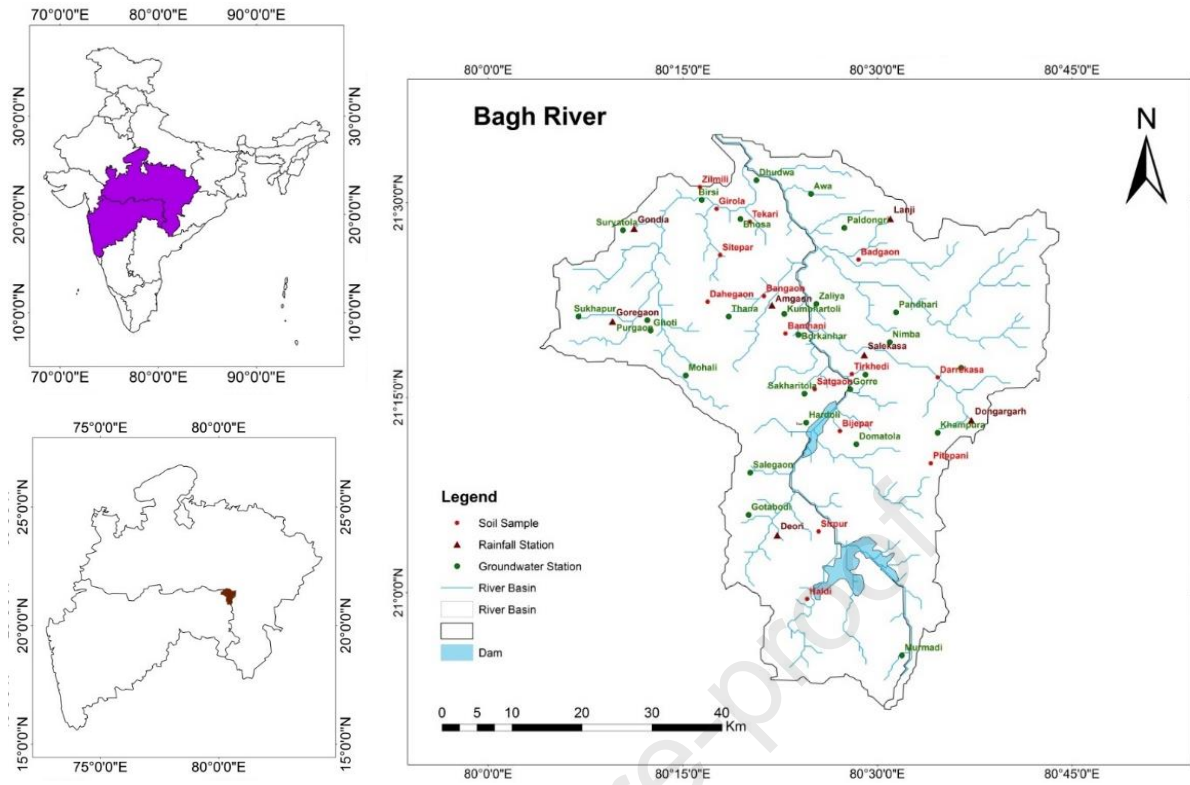
183 **2.2. Computation of the Water Quality Index (WQI)**

184 The evaluation of groundwater quality for irrigation purposes is based on the WQI,
185 which is frequently used to evaluate water quality and its suitability for agricultural use [3,35].
186 The WQI is a comprehensive rating system that considers various water quality variables and
187 condenses them into a single overall rating, representing the overall water quality. In this
188 study, ten significant characteristics were considered to compute the WQI. The first phase
189 necessitates giving unit weights to each physicochemical parameter using a "weighted
190 arithmetic index" to normalize the parameters with different units and dimensions onto a
191 comparable scale [36].

192

193

194



195 **Fig. 1.** Case study river basin showing the location of water sample collected and river basin
 196 drainage networks.

197 The proportional weights for each parameter were determined based on their unit
 198 weights. The quality rating was computed by comparing each parameter's observed
 199 concentration and norm concentration. The sub-index was then produced by multiplying the
 200 quality rating of each parameter by the appropriate relative weight. The WQI, which was the
 201 result of adding the sub-indices for each attribute, was then developed. More details about
 202 the assigned weights (W_i), relative weights (w_i), and the WHO standard are provided in Table
 203 1 [37]. The assigned weights (W_i), is calculated using equations (1) given below:

$$204 \quad W_i = \frac{w_i}{\sum_{i=1}^n w_i} \quad (1)$$

205 A quality rating scale (q_i) is calculated for each parameter by using the equation (2) given as:

$$206 \quad q_i = \left(C_i / S_i \right) \times 100 \quad (2)$$

207 Additionally, a subindex of the i^{th} parameter is estimated based on equation (3) given as:

$$208 \quad SI_i = q_i \times W_i \quad (3)$$

209 Lastly, the water quality index is calculated using the equation (4) given as:

$$210 \quad WQI = \sum SI_i \quad (4)$$

211 where W_i = relative weight, w_i = weight/parameter, n = number of parameters, C_i =
 212 chemical concentration per water sample (mg/L), S_i = quality standard for drinking water as
 213 per WHO (mg/L), SI_i = subindex rating, q_i = quality rating and W_i = relative weight

214 **Table 1:** Weight of parameters and their standard for WQI

Chemical parameters	Standards (BIS 2003; [37])	Weight (w_i)	Relative weight (W_i)
Sulphate (SO_4^{2-})	200	5	0.114
Nitrate (NO_3^-)	45	5	0.114
Fluoride (F^-)	1	5	0.114
Chloride (Cl^-)	250	5	0.114
Total dissolved solids (TDS)	500	5	0.114
Sodium (Na^+)	50	5	0.114
pH	8.5	3	0.068
Calcium (Ca^{2+})	75	3	0.068
Magnesium (Mg^{2+})	30	3	0.068
Potassium (K^+)	100	2	0.045
Total hardness (TH)	300	2	0.045
Bicarbonate (HCO_3^-)	200	1	0.023
		$\Sigma w_i = 44$	$\Sigma W_i = 1$

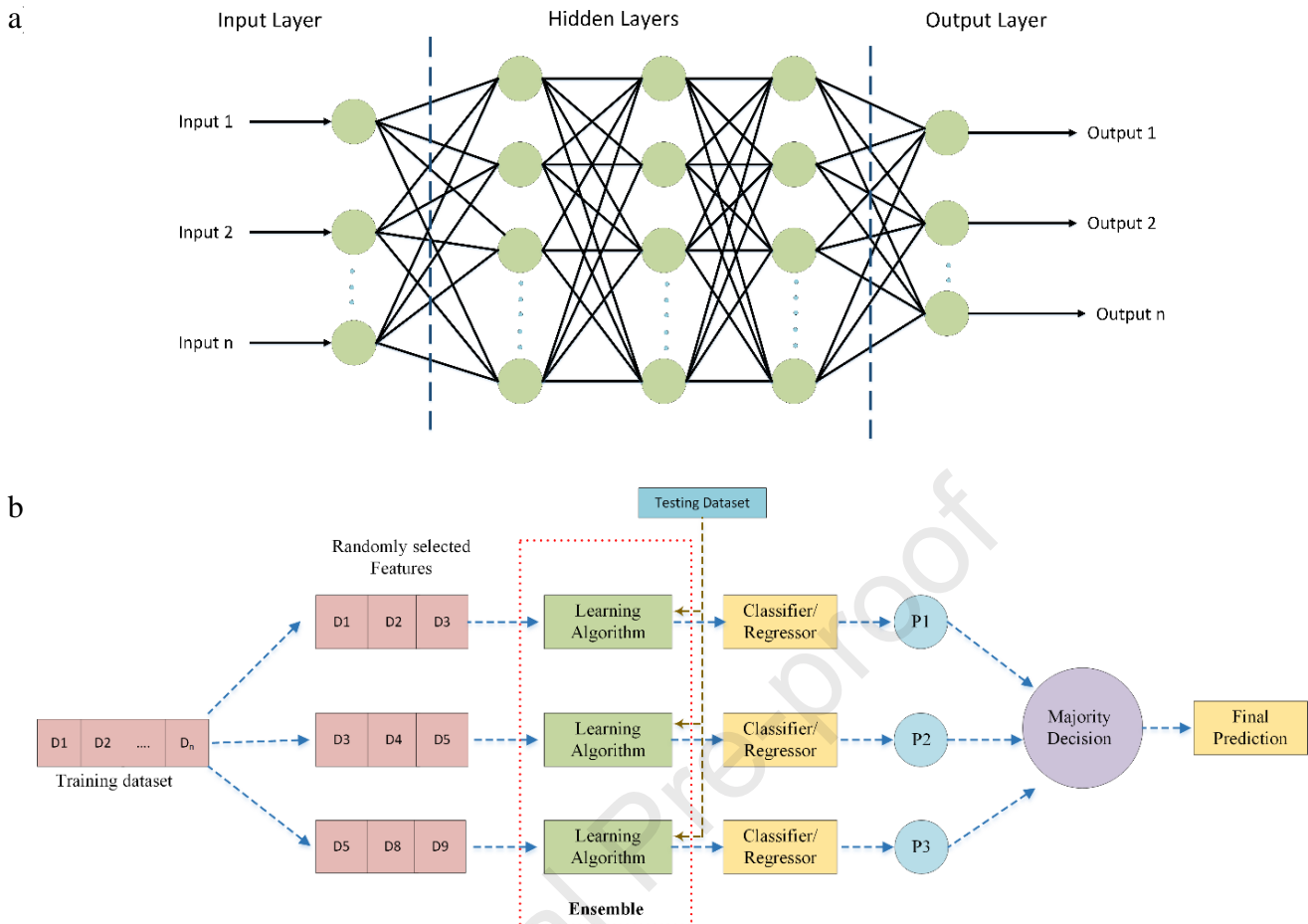
Note: All concentrations in given mg/L excluding pH

215

216 **2.3. Machine learning algorithms**

217 **2.3.1. Artificial neural network (ANN)**

218 Artificial Neural Network (ANN) is a computational modeling tool containing
 219 interconnected adaptive dispensation rudiments, capable of executing massive parallel
 220 computations for complex data processing and knowledge representations [38–40]. In the
 221 past few decades, research into ANNs has shown explosive growth, covering various
 222 applications in various areas. ANN models follow an exact planning, which the biological
 223 nervous system enthuses. Like the human brain, the ANN model comprises neurons arranged
 224 in a complex nonlinear form in a layered fashion, and the neurons in adjacent layers are
 225 interconnected by weighted links [41]. Each input is multiplied by its appropriate weights after
 226 being received by the input layer of the ANN in the form of text, numeric, or picture vectors.
 227 These weights often reflect how strongly the ANN's neurons are connected. The middle,
 228 hidden layer(s) performs mathematical computations to extract patterns from the input data.
 229 The hidden layer's meticulous computations enable the ANN to produce the desired result in
 230 the output layer. The architecture of ANN is shown in Fig. 2a. Ideally, ANNs are trained with
 231 large datasets to derive meaningful insights and patterns from the dataset [42].



232 **Fig. 2.** Schematic diagram of (a) ANN (b) Random subspace method.

233

234 2.3.2. Random subspace (RSS)

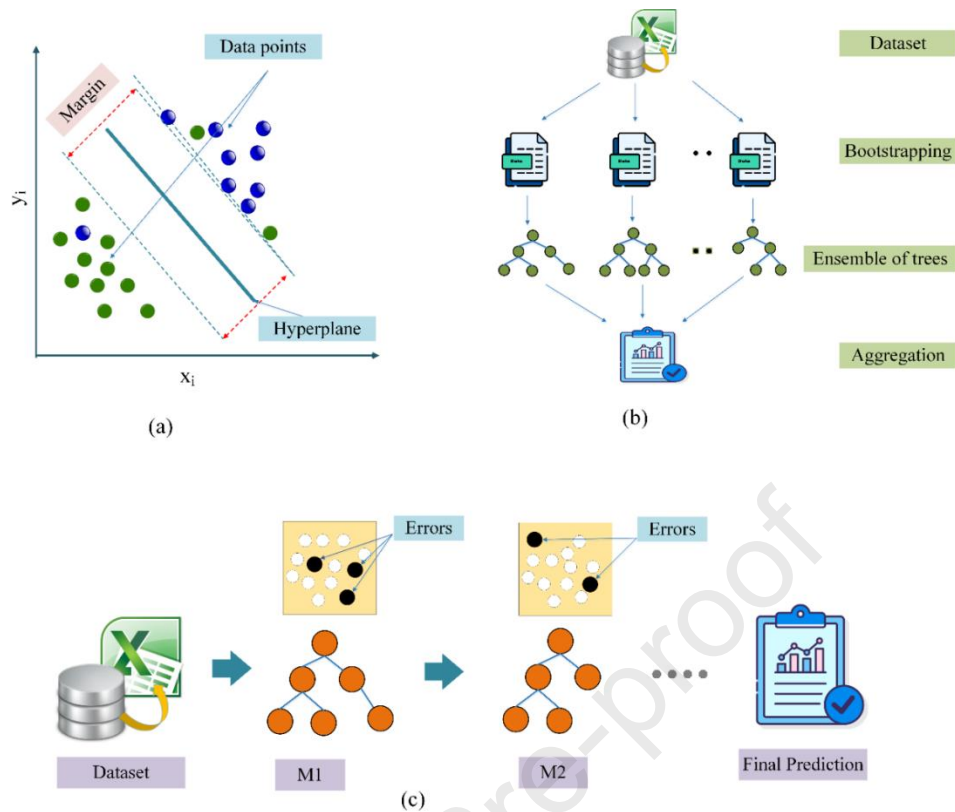
235 The random subspace algorithm is a machine learning ensemble method that enhances
 236 diversity among ensemble learners by limiting the models to operate on various random
 237 subsets of the entire feature space [43,44]. The general layout of RSS is presented in Fig. 2b.
 238 The issue of very large dimensionality is elegantly solved with RS ensembles. Smaller
 239 subspaces make it easier to train the predictors and significantly increase the feature-to-
 240 instance ratio [45]. When there are few training items in proportion to the amount of data,
 241 RSS is extremely useful. Furthermore, random subspace offers stronger predictors when data
 242 contains many redundant features than the original feature space. The first phase entails
 243 predicting the initial space into subsets, and in the final stage, the result obtained is
 244 aggregated through voting or averaging [46].

245 2.3.3. Support vector machine (SVM)

246 Supervised learning is a popular classification method, and regression and outlier
247 detection is the support vector machine. The classification job serves as the greatest lens to
248 comprehend the SVM algorithm. In an N-dimensional space, the SVM classifier creates a
249 hyperplane that divides the data points into different classes [47–49]. The margin is used to
250 choose the hyperplane. In other words, the hyperplane with the largest margin between the
251 classes is picked. Support vectors-data points closer to the hyperplane are used to determine
252 these margins. SVM can be well utilized as a regression approach, maintaining all the key
253 topographies that describe the algorithm (maximal margin). SVM is well suited for regression
254 issues due to its sparse solution and stronger generalization ability (Fig. 3a). A new ε -
255 insensitive region, known as ε -tube generated around the function, helps approximate the
256 continuous-valued function and reduces the prediction error. Like SVM classifiers, the support
257 vectors are the most important factors affecting how the tube is shaped in SVR. SVR also
258 counts on the independence and identical distribution of the training and testing sets of the
259 data [50].

260 **2.3.4. Random forest (RF)**

261 The popular and adaptable supervised machine learning technique Random Forest is
262 effective for classification and regression issues. The core idea behind RF is to grow and
263 combine multiple decision trees to form a “forest.” All choice tree in a random forest is trained
264 on a subset of data, and the contribution of individual trees gives stability to the algorithm
265 and reduces the variance [51,52]. The algorithm creates individual trees from different input
266 data samples; further, at each bulge, dissimilar samples of topographies are designated for
267 excruciating. The trees run in similar deprived of any interaction, and finally, the prediction
268 from individual trees is averaged to produce the final result for the random forest regressor
269 prediction. RF replicas have remained proven to be robust forecasters for both small datasets
270 and higher dimensional data [53]. RF exhibits better generalization and tends to outpace most
271 additional methods in footings of their performance, deprived of overfitting. Compared to
272 decision trees, RF is more robust to noise in the dataset, and hyperparameter tuning is
273 relatively easy [54]. The general layout of RF is presented in Fig. 3b.



274
 275 **Fig. 3.** Schematic diagram of (a) SVM, (b) Random Forest, and (c) Additive Regression
 276 models.

277 2.3.5. Additive regression (AR)

278 The additive regression model performs stage-wise addition, and new learners are
 279 extra one at a period by freezing the existing learners. i.e., the previous learners are left
 280 unchanged. A collaborative of feeble regression prediction models, often decision trees, is
 281 produced by additive regression as a prediction model. The additive regression trees are very
 282 similar to the gradient boosting trees, wherein contributions of sequential weak learners are
 283 strengthened at each iteration. In every iteration, it fits a model to the residuals of the
 284 previous iteration. The model's residuals are used for training, which gives the incorrectly
 285 predicted data more weight. Additionally, each weak learner's contribution to the final
 286 prediction is based on a gradient optimization technique to lower the overall error of the
 287 strong learner.

288 The overfitting is prevented by reducing the learning rate parameter and providing a
 289 smoothing effect [55]. With vast and complex datasets, these additive regression stands out
 290 for their accurate prediction capabilities [56]. The architecture of AR is shown in Fig. 3c.

291 **2.3.6. M5 Pruned (M5P)**

292 The M5 tree algorithm, introduced by Quinlan [57] is a choice tree with linear
293 regression at the leaf nodes, that can help predict incessant arithmetical qualities. The M5P
294 algorithm is simple to apply and gives more comprehensible linear mathematical equations
295 among the contribution and yield variables when likened to additional machine learning
296 algorithms. The model efficiently predicts continuous values and can handle data with higher
297 dimensionality. The computation of error at each node provides the basis for determining the
298 excruciating standard for the M5P model tree. The error is analyzed based on the standard
299 deviation of the standards at a particular node. The data in child nodes are purer and have a
300 lower standard deviation than that of the parent node due to the splitting process. The model
301 evaluates each alternative split, choosing the one that minimizes errors while maximizing
302 error reduction [58]. This approach often creates a huge tree-like structure that could lead to
303 overfitting. The overgrown trees are pruned to tackle this overfitting by relieving the sub-
304 trees with linear regression functions [59].

305

306 **2.3.7. Selection of best input combination for model development**

307 The best performance of the selected models depends on carefully selecting the water
308 quality input parameters during the water quality modeling process. Numerous combinations
309 of these parameters were utilized to find the ideal input combination. Then, using the Relief
310 method, a certain combination was found to be the best [60]. The relief algorithm has
311 emerged as a widely adopted technique for feature selection. Its primary objective is to assess
312 the significance of individual features within a dataset by gauging their capacity to
313 differentiate between distinct classes. The operational principle of this algorithm revolves
314 around attributing weights to each feature, predicated on their effectiveness in distinguishing
315 between neighboring instances within the feature space [61]. The algorithm's functionality
316 can be summarized as follows: It assigns weight values to features based on their aptitude for
317 discriminating among closely situated data points within the feature space. These weight
318 values subsequently undergo a prioritization process, leading to the ranking of features based
319 on their perceived importance. Features that attain higher ranks are deemed more pertinent
320 in contributing to the differentiation of classes. Utilizing the relief algorithm confers multiple
321 advantages, notably in scenarios where the novel dataset includes many structures. By

322 electing to retain the most pertinent features according to the algorithm's ranking, it becomes
323 possible to enhance the correctness and efficacy of machine learning models. This is
324 predominantly beneficial in situations where the volume of features might otherwise
325 introduce complexity and resource-intensive computations [3,62]. Among 12 independent
326 input variables, i.e., pH, HCO_3^- , Cl^- , NO_3^- , TDS, TH, Ca^{2+} , Mg^{2+} , Na^+ , K^+ , SO_4^{2-} and F^-), the five
327 most influencing variables were selected for model development. These include NO_3^- , SO_4^{2-} ,
328 Ca^{2+} , Mg^{2+} , and K^+ . Fig. 4 presents the ranks of the selected variables for predicting the WQI.

329 **2.3.8. Fusion of meta-heuristic algorithms through stacked generalization**

330 Stacked hybridization, also known as stacked ensemble learning, is a machine learning
331 technique that combines multiple diverse machine learning models to improve predictive
332 performance [63]. This approach leverages the strengths of individual models and mitigates
333 their weaknesses by training a meta-model, or a "stacked" model, on the predictions made
334 by these base models. The stacked model learns how to weigh the predictions from each base
335 model to make a final prediction, often resulting in improved accuracy, robustness, and
336 generalization. Research findings indicate that using stacked hybrid algorithms can enhance
337 the predictive capabilities of these algorithms [64,65]. Stacked hybridization allows you to
338 take advantage of the diverse strengths of different models, potentially leading to improved
339 predictive performance compared to using any single model in isolation. However, it's
340 essential to perform careful model selection, tuning, and validation to ensure the success of
341 a stacked ensemble. The steps involved in the stacked hybridization of an Artificial Neural
342 Network (ANN) with another machine learning algorithm, such SVM, are outlined below:

343 **Step 1:** Begin by selecting two base models: base model 1, which is the ANN, and base model
344 2, which is the SVM.

345 **Step 2:** Split the training data into two sets: training the ANN and SVM (the first-level training
346 data) and training the stacked model (the second-level training data).

347 **Step 3:** Train the ANN using the first-level training data while adjusting the neural network's
348 architecture and parameters. Simultaneously, train the SVM using the first-level training data
349 while optimizing the kernel and hyperparameters.

350 **Step 4:** Employ the trained ANN and SVM to make predictions on a validation or holdout
351 dataset.

352 **Step 5:** Train a meta-model, such as logistic regression or a decision tree, utilizing the
 353 predictions generated by the ANN and SVM on the validation dataset. This meta-model is
 354 designed to learn how to effectively combine these predictions.

355 **Step 6:** For making predictions on new data, apply both the ANN and SVM to generate
 356 predictions. Then, employ the trained meta-model to combine these predictions, resulting in
 357 the final prediction.

358 **2.4. Evaluation of the statistical performance of hybrid model developments**

359 The evaluation of the performance of the computed Water Quality Index (WQI) and
 360 predicted WQI using hybrid models involved the utilization of commonly recognized statistical
 361 metrics. These metrics encompass the Nash-Sutcliffe efficiency (NSE), Pearson correlation
 362 coefficient (PCC), Coefficient of determination (R²), Mean absolute error (MAE), Root mean
 363 square error (RMSE), Relative root square error (RRSE), Relative absolute error (RAE), and
 364 Mean Bias Error (MBE). These metrics have been effectively employed to assess model
 365 performance in previous studies [66–69]. The RMSE is employed to quantify the disparity
 366 between expected and observed values within a time series. RRSE, as the square root of
 367 relative squared error, minimizes errors in dimensions that match the predicted quantity.
 368 MAE describes the mean absolute deviation of anticipated time series values from observed
 369 values. RAE assesses the absolute error's magnitude relative to the measurement's size and
 370 displays the ratio of absolute error to the actual measurement. Nash-Sutcliffe efficiency is a
 371 widely used statistic for evaluating model performance, ranging from 1, indicating an ideal fit,
 372 to -1. A value of 0 implies accuracy equivalent to the mean value.

373 On the other hand, the coefficient of determination (R²) quantifies the linear relationship
 374 between dependent and independent variables. In the context of WQI modeling, models with
 375 higher R² values (closer to 1), higher RRSE values, and lower values of MBE, RMSE, MAE, and
 376 RAE are considered superior. In the equations (5-11), the WQI_C and WQI_P represent the
 377 computed/observed and predicted or simulated values for the i^{th} dataset, while WQI_{avg} and
 378 WQI_{pavg} denote the average or mean magnitude of observed and predicted or simulated
 379 values. N signifies the number of observations.

$$380 \quad MBE = \frac{1}{N} \sum_{i=1}^N (WQI_P - WQI_C) \quad (5)$$

$$381 \quad RMSE = \sqrt{\frac{1}{N} \sum_{i=1}^N (WQI_C - WQI_P)^2} \quad (6)$$

$$382 \quad RRSE = \sqrt{\frac{\sum_{i=1}^N (WQI_C - WQI_P)^2}{\sum_{i=1}^N (WQI_C - WQI_{cavg})^2}} \quad (7)$$

$$383 \quad MAE = \frac{1}{N} \sum_{i=1}^N |WQI_C - WQI_P| \quad (8)$$

$$384 \quad RAE = \frac{\sum_{i=1}^N |WQI_C - WQI_P|}{\sum_{i=1}^N |WQI_C - WQI_{cavg}|} \quad (9)$$

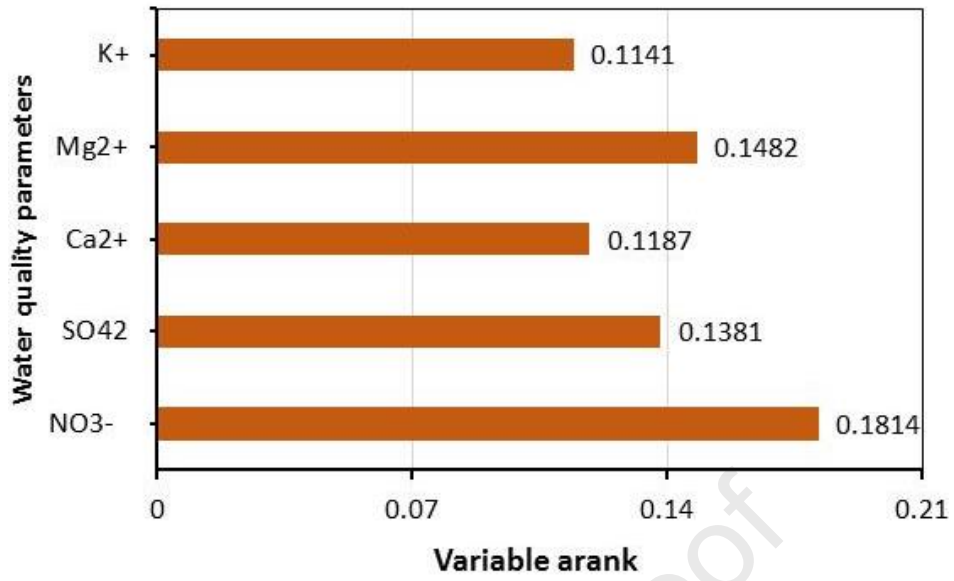
$$385 \quad R^2 = 1 - \frac{\sum_{i=1}^N (WQI_C - WQI_P)^2}{\sum_{i=1}^N (WQI_C - WQI_{cavg})^2} \quad (10)$$

$$386 \quad NSE = 1 - \left[\frac{\sum_{i=1}^N WQI_C - WQI_P}{\sum_{i=1}^N (WQI_C - WQI_{cavg})} \right]^2 \quad (11)$$

387 **3. Results**

388 **3.1. Dominance analysis and relative importance of water quality parameters**

389 The dominance analysis of water quality input parameters uses the Relief algorithm
 390 [60]. Fig. 4 presents the ranks of the selected variables (i.e., NO_3 , Mg^{2+} , SO_4^{2-} , Ca^{2+} , and K^+)
 391 from 12 water quality parameters (i.e., pH, HCO_3^- , Cl^- , NO_3 , TDS, TH, Ca^{2+} , Mg^{2+} , Na^+ , K^+ , SO_4^{2-}
 392 and F) for predicting the WQI. The detailed analysis of the chemical composition of water
 393 quality is summarized in Table 2. The values of pH ranged from 6.60 to 8.92 with an average
 394 of 7.73 ± 0.52 ; TDS varies from 241 to 2100 with an average of 678 ± 469.94 and 30.0 to 681.0
 395 with an average of 246.54 ± 176.98 for TH. Among cations, their concentration ranged from
 396 7.80 to 680.0 with an average of 293.65 ± 193.43 for Na^+ ; 0.20 to 411.0 with an average of
 397 57.58 ± 106.76 for K^+ ; 1.20 to 241.0 (100.16 ± 74.46) for Ca^+ , and 1.22 to 161.24 with an average
 398 of 51.70 ± 47.82 for Mg^+ . However, their anion attentiveness alternated from 14.0 to 3014.80
 399 with an average of 472.67 ± 615.08 for Cl^- ; 128.0 to 652.0 with a normal of 293.65 ± 123.01 for
 400 HCO_3^- and 6.0 to 481.0 with an average of 75.07 ± 127.95 for SO_4^{2-} . In footings of anions,
 401 Chloride is the maximum predominant, shadowed by Bicarbonate and Chlorine. The
 402 weightage of selected water quality parameters for WQI prediction has been shown in Fig. 4.
 403



404

405

406

Fig. 4. Weightage of selected variables for model development.

407

Table 2: Statistical summary of water quality parameters

Parameters	Mean	SD	Skewness	Kurtosis	Minimum	Maximum	Range	WHO (1997)		BIS (2003) (IS 10500)	
								Maximum desirable	Highest permissible	Maximum desirable	Highest permissible
pH	7.73	0.52	-0.12	0.60	6.60	8.92	2.32	7.0-8.5	6.5-9.2	6.5-8.5	8.5-9.2
TDS	678.00	469.94	1.98	4.39	241.00	2100.00	1859.00	500	1500	500	2000
TH	246.54	176.98	1.09	0.91	30.00	681.00	651.00	100	500	300	600
Ca ⁺²	100.16	74.46	0.54	-0.82	1.20	241.00	239.80	75	200	75	200
Mg ⁺²	51.70	47.82	1.05	0.28	1.22	161.24	160.02	30	150	30	100
Na ⁺	293.65	193.43	0.43	-0.72	7.80	680.00	672.20	50	200	-	-
K ⁺	57.58	106.76	3.09	8.85	0.20	411.00	410.80	100	200	-	-
HCO ₃ ⁻	293.65	123.01	1.72	4.51	128.00	652.00	524.00	200	600	200	600
Cl ⁻	472.67	615.08	3.02	11.65	14.00	3014.80	3000.80	250	600	250	1000
No ₃ ⁻	61.38	197.66	4.13	18.28	0.11	957.80	957.69	-	50	45	100
SO ₄ ⁻²	75.07	127.95	2.70	6.96	6.00	481.00	475.00	200	600	200	400
F ⁻	0.97	0.70	0.04	-1.36	0.06	2.10	2.04	0.6-1.5	1.5	1.0	1.5

Note: All concentrations in mg/L, excluding pH

408

409 3.2. Prediction of water quality index (WQI)

410 The primary objective of this study is to create innovative hybrid machine learning
 411 algorithms/models and assess their predictive capabilities for the Water Quality Index (WQI)
 412 in the Bagh River Basin (BRB). This section presents the outcomes of modeling WQI using data-
 413 driven hybrid machine-learning algorithms. We evaluated the performance of the Artificial
 414 Neural Network (ANN) and its hybridization with five other machine learning algorithms:
 415 ANN-RF, ANN-SVM, ANN-RSS, ANN-AR, and ANN-M5P, for WQI prediction.

416 3.2.1 Development of models and their training

417 We investigated the enhancement of artificial neural networks (ANN) through stacked
 418 hybridization with other machine learning algorithms to improve water quality prediction.
 419 Water quality parameters, notably K^+ , Ca^{2+} , SO_4 , Mg^{2+} , and NO_3^- , were identified as the most
 420 influential input factors for WQI prediction. To assess the performance of the hybridized
 421 models relative to the conventional ANN, we employed eight statistical indicators to evaluate
 422 each model's effectiveness. The results obtained during the training phase are summarized in
 423 Table 3.

424 **Table 3.** Statistical indices of the proposed hybrid models during the training

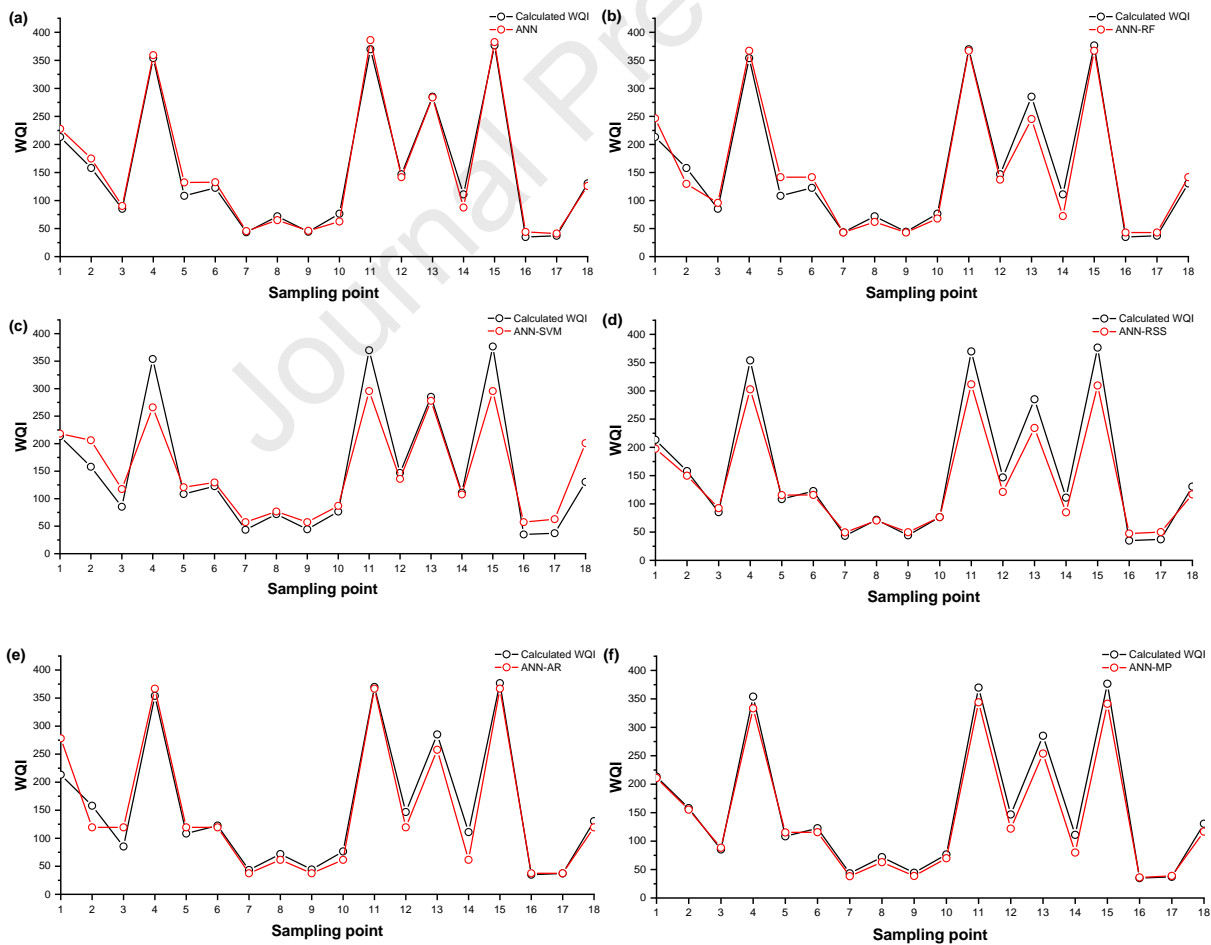
Statistical indices	ANN	ANN-RF	ANN-SVM	ANN-RSS	ANN-AR	ANN-M5P
PCC	0.996	0.984	0.956	0.996	0.977	0.996
R ²	0.991	0.968	0.913	0.992	0.954	0.992
MAE	9.435	15.777	29.431	20.889	18.558	13.029
MBE	3.289	-0.850	0.000	-15.223	-4.556	-11.608
RMSE	11.695	20.229	40.961	29.332	25.583	17.351
RAE (%)	10.185	17.032	31.772	22.551	20.034	14.065
RRSR (%)	10.302	17.821	36.083	25.839	22.536	15.285
NSE	0.989	0.968	0.870	0.933	0.949	0.977

425
 426 Table 3 illustrates that the ANN model did remarkably well to predict training results
 427 during the prediction phase, as the Pearson's correlation coefficient (PCC) for ANN was 0.996.
 428 The performance indicators showed the smallest values with an MAE = 9.435, MBE = 3.289,
 429 RMSE = 11.695, RAE (%) = 10.185 and RRSR (%) = 10.302, and the highest value of NSE for
 430 ANN was 0.989. It was trailed straight by the ANN-M5P model which had a Pearson's
 431 correlation coefficient of PCC = 0.996, smallest values of MAE = 13.029, MBE = -11.608, RMSE

432 = 17.351, RAE (%) = 14.065 and RRSR (%) = 15.285. The highest value of NSE for ANN-M5P was
 433 0.977, while the nethermost accomplishment model in the exercise stage was the ANN-SVM
 434 model with Pearson's correlation coefficient (PCC) = 0.956, and smallest values of MAE =
 435 29.431, MBE = 0.000, RMSE = 40.961, RAE (%) = 31.772 and RRSR (%) = 36.083, and the highest
 436 value of NSE for ANN-SVM was 0.870. Grounded on the numerical presentation indicators
 437 acquired throughout the exercise phase of all seven models, it was obvious that they
 438 performed well.

439 This further demonstrated that in the training data sets, the ANN model outperformed
 440 the ANN-M5P, ANN-RF, ANN-AR, ANN-RSS, and ANN-SVM models in predicting WQI. During
 441 the training phase, the ANN-SVM model performs noticeably poorer at predicting the WQI.
 442 The top four models, ANN, ANN-M5P, ANN-RF, and ANN-AR, were chosen to forecast WQI
 443 because of their excellent precision and accuracy.

444

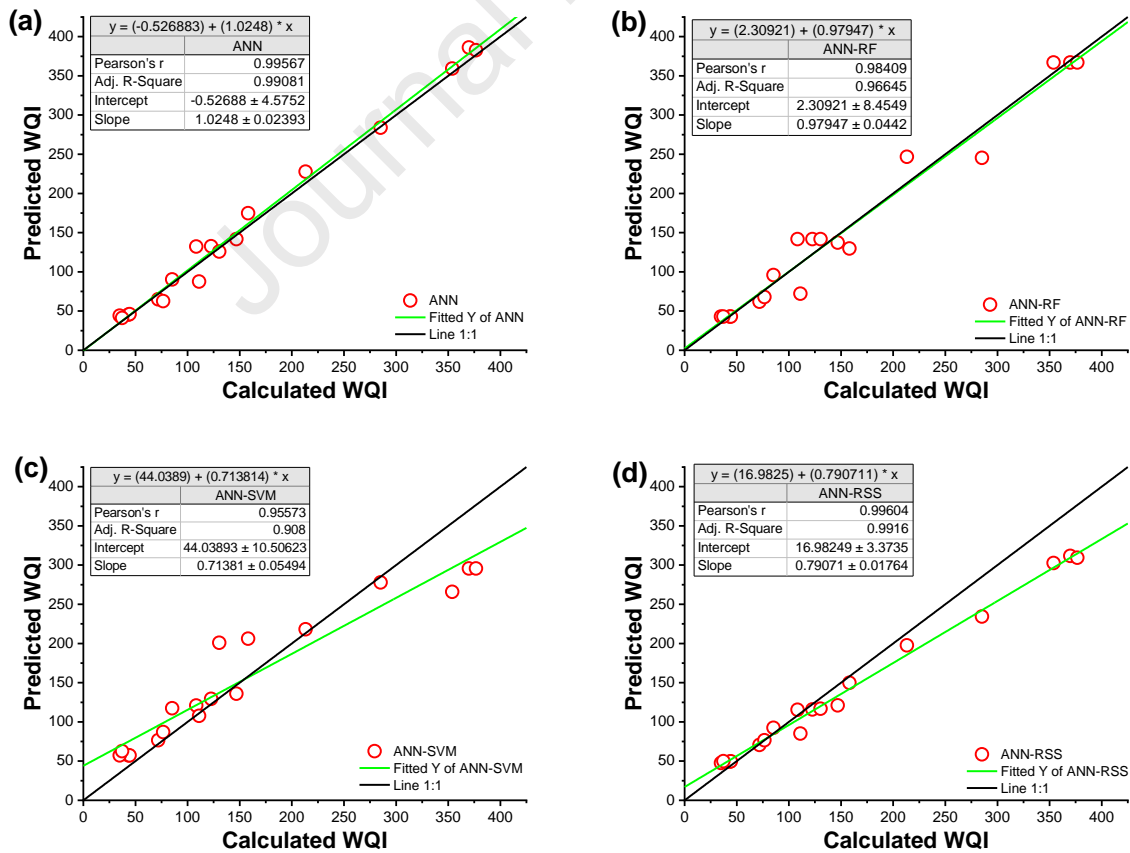


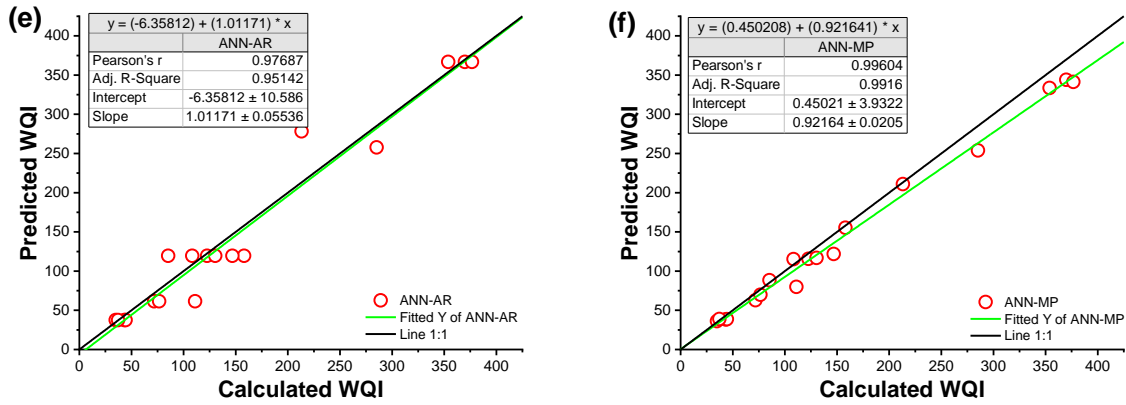
445 **Fig. 5.** Line diagram of computed and predicted WQI for training data sets for (a) ANN
 446 stand-alone, (b) ANN-RF, (c) ANN-SVM (d) ANN-RSS, (e) ANN-AR, and (f) ANN-M5P

447 In the training phase, the contrast between observed and predicted WQIs was
 448 presented using time series and scatter plots to illustrate the comparison between observed
 449 and predicted WQI based on the selected models (Fig. 5 and 6). In Fig. 5, the simulations by
 450 ML models (continuous red line with circle symbol) are compared with the calculated WQI
 451 (continuous black line with circle symbol). The period sequence in this study was constructed
 452 from the time series generated by all sampling sites based on the training data set. Statistical
 453 parameters (i.e., MBE), line diagram (Fig. 5), and scatter plot (Fig. 6) show that the ANN was
 454 slightly over-predictive than the others.

455 When all the model's values are evenly spaced along or on either side of the 1:1 line,
 456 suggesting errors in the data, that model is shown to be accurate. In contrast to the values
 457 predicted by the ANN-RF, ANN-SVM, ANN-RSS, ANN-AR, and ANN-M5P models, which are all
 458 dispersed under the 1:1 line, the values predicted by the ANN model ($R^2 = 0.991$) are more
 459 equally distributed over the 1:1 line. ANN-SVM and ANN-RSS are shown to be more under-
 460 predictive than others.

461





462 **Fig. 6.** Scatter plot of computed and predicted WQI for training data sets (a) ANN stand-
 463 alone, (b) ANN-RF, (c) ANN-SVM (d) ANN-RSS, (e) ANN-AR, and (f) ANN-M5P

464 Our analysis of the performance values of the indicators showed that the eight
 465 models, on the whole, perform at an acceptable level. Yaseen et al. [13] and Markuna et al.
 466 [70] found that the RMSE is one of the most significant quantitative indicators of model
 467 performance during any analysis of data-mining models and time series data forecasting since
 468 it is one of the most predictive indicators.

469 3.2.2 Validation of applied ML algorithms

470 Table 4 provides a summary of the results obtained during the validation phase.
 471 Among the models tested, the ANN model displayed the highest correlation and the lowest
 472 error during the training phase. However, its performance with the test datasets was
 473 suboptimal. On the other hand, the proposed hybrid ANN-SVM model exhibited the lowest
 474 error indicators and the highest Pearson's correlation coefficient (PCC = 0.951) during the
 475 validation phase. Notably, it achieved high values for NSE (0.879), PCC (0.951), and R^2 while
 476 demonstrating low values for MAE (22.349), MBE (12.548), RMSE (27.974), RAE (30.039%),
 477 and RRSR (34.227%). These results indicate that the ANN-SVM model effectively recognized
 478 the WQI pattern and provided accurate predictions.

479 The ANN model closely follows the top-performing analytical model, ANN-SVM. The
 480 ANN model achieved high values for NSE (0.842), PCC (0.923), and R^2 (0.852) and displayed
 481 low values for MAE (18.362), MBE (-7.944), RMSE (31.923), RAE (24.680%), and RRSR
 482 (39.059%). Additionally, the ANN-M5P model exhibited strong performance with high NSE
 483 (0.782), PCC (0.927), R^2 (0.859), and low MAE (22.261), MBE (-20.579), RMSE (37.499), RAE
 484 (29.920%), and RRSR (45.881%). In contrast, the ANN-RF model showed less favorable test

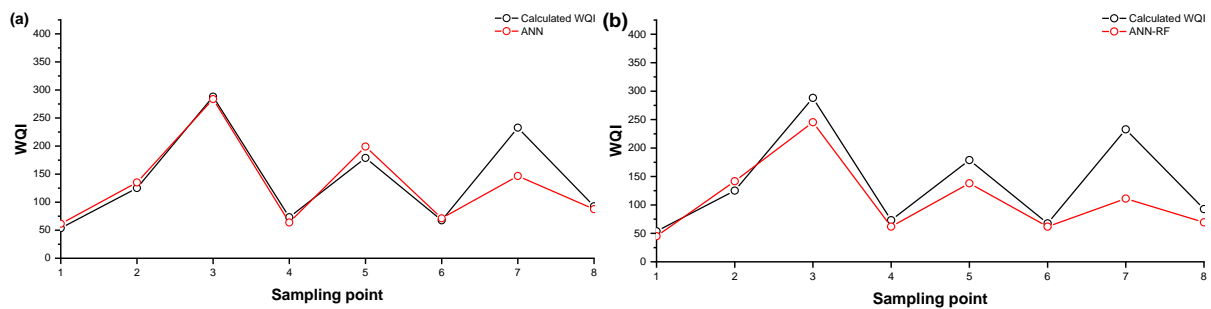
485 results with $PCC = 0.880$, $R^2 = 0.774$, $MAE = 33.855$, $MBE = -29.733$, $RMSE = 49.224$, $RAE (\%) =$
 486 45.502 , and $RRSR (\%) = 60.228$, along with an NSE of 0.625 . These results clearly indicate that
 487 the ANN-SVM model outperformed the ANN, ANN-M5P, ANN-RSS, ANN-AR, and ANN-RF
 488 models in predicting WQI for the test datasets. The noticeably poorer performance of the
 489 ANN-RF model during the testing phase suggests that the inconsistent quality of the test
 490 dataset may have contributed to its subpar results.

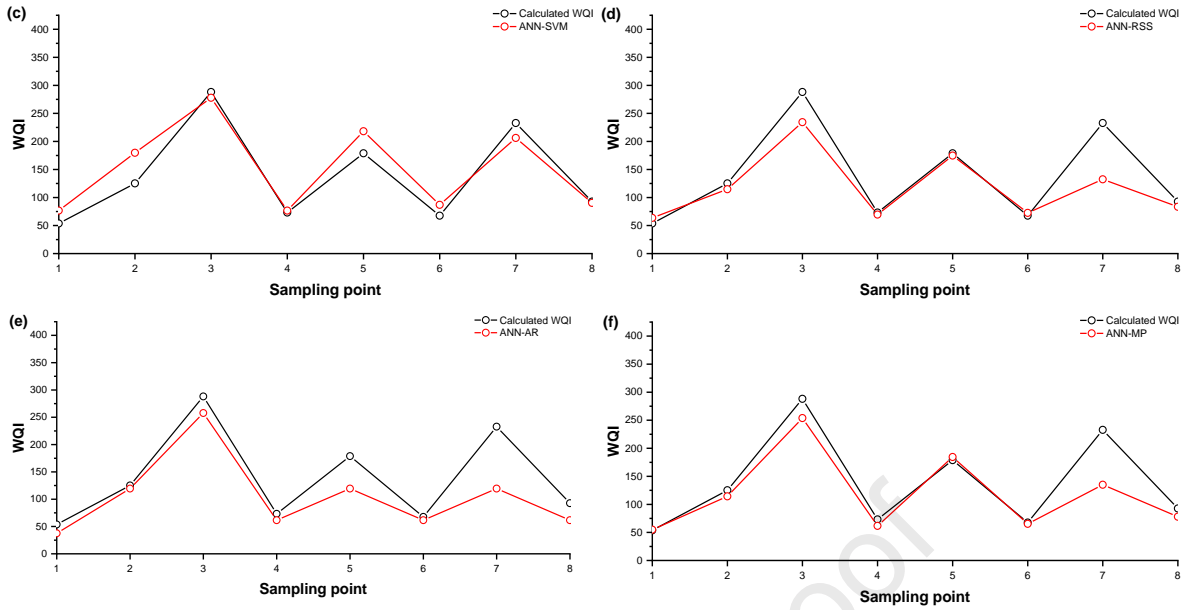
491 **Table 4.** Statistical indices of the proposed model in the testing datasets.

Statistical indices	ANN	ANN-RF	ANN-SVM	ANN-RSS	ANN-AR	ANN-M5P
PCC	0.923	0.880	0.951	0.927	0.910	0.927
R^2	0.852	0.774	0.904	0.859	0.828	0.859
MAE	18.362	33.855	22.349	24.552	34.247	22.261
MBE	-7.944	-29.733	12.548	-20.809	-34.247	-20.579
RMSE	31.923	49.224	27.974	40.804	48.405	37.499
RAE (%)	24.680	45.502	30.039	32.999	46.029	29.920
RRSR (%)	39.059	60.228	34.227	49.925	59.226	45.881
NSE	0.842	0.625	0.879	0.742	0.637	0.782

492

493 To visualize the disparities between observed and predicted WQI based on the
 494 selected models, we compared them using time series and scatter plots during the validation
 495 phase (Fig. 7 and 8). In Fig. 7, the simulations by ML models (represented by the continuous
 496 red line with circle symbols) were contrasted with the computed WQI (shown as the
 497 continuous black line with circle symbols). The time series used in this study was constructed
 498 from data generated by all sampling sites based on the testing dataset.

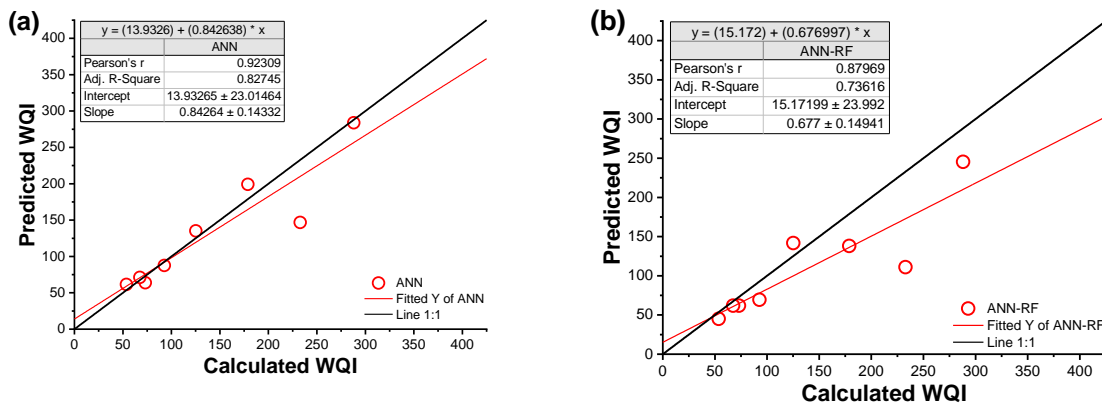


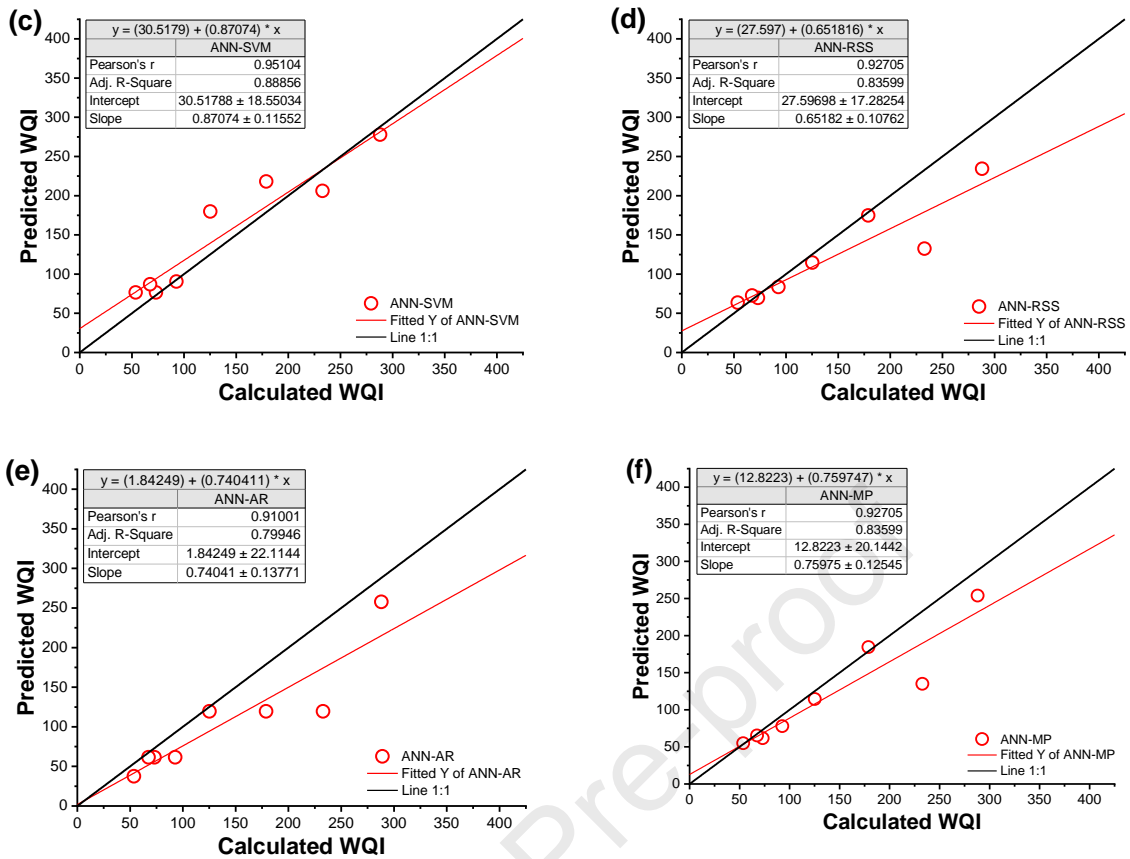


499 **Fig. 7.** Line diagram of computed and predicted WQI for testing data sets for (a) ANN stand-
 500 alone, (b) ANN-RF, (c) ANN-SVM (d) ANN-RSS, (e) ANN-AR, and (f) ANN-M5P

501 Statistical parameters, such as MBE, along with the line diagram (Fig. 7) and scatter
 502 plot (Fig. 8), indicated that the ANN-SVM model exhibited a slightly higher level of over-
 503 prediction than the other models. An accurate model typically exhibits an even distribution
 504 of values on or around the 1:1 line, signifying a balanced representation of errors. However,
 505 the values predicted by the ANN-SVM model ($R^2 = 0.904$) were notably more evenly
 506 distributed along the 1:1 line compared to the predictions of the ANN, ANN-RF, ANN-RSS,
 507 ANN-AR, and ANN-M5P models, which all showed a dispersion below the 1:1 line, as evident
 508 in Fig. 8. Except for ANN-SVM model, all other models tended to under-predict the observed
 509 values.

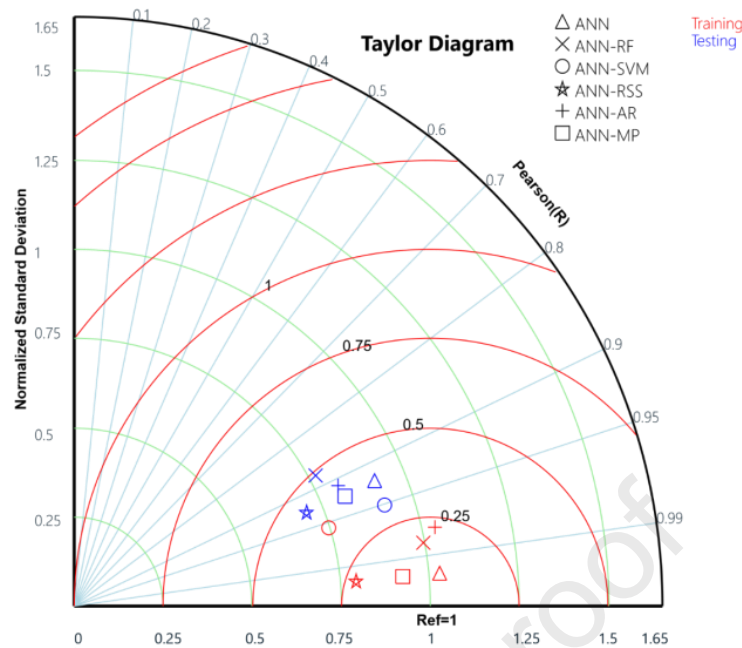
510





511 **Fig. 8.** Scatter plot of computed and predicted WQI for testing data sets for (a) ANN stand-alone,
 512 (b) ANN-RF, (c) ANN-SVM (d) ANN-RSS, (e) ANN-AR, and (f) ANN-M5P

513 In addition, a Taylor diagram was employed to assess the model's performance, as
 514 introduced by [71]. Fig. 9 illustrates that the ANN-SVM and ANN-RF models stood out among
 515 the other hybrid models as they were positioned farthest from the computed or reference
 516 WQI values during the training and validation phases, respectively. The ANN standalone and
 517 ANN-SVM models were found closest to the reference point during the training and validation
 518 phases, respectively. Taylor diagram considers factors such as standard deviation (SD),
 519 correlation (PCC), and root mean square error (RMSE) of the model. It is worth noting that
 520 the most effective model is the one that excels in predicting the test dataset, as demonstrated
 521 in previous studies [31,66,68,72]. Furthermore, this reaffirms that SVM algorithms enhance
 522 the performance of ANN through hybrid models and prove to be superior to all other hybrid
 523 and standalone ANN models for predicting WQI in the Bagh River Basin, India.



524

525 **Fig. 9.** Taylor diagram showing comparative performance of developed hybrid models526 **4. Discussion**

527 As detailed above, Sections 3.1 and 3.2 describe the WQI prediction results and the
 528 key factors that significantly influence the water quality that we have selected for the present
 529 study. These factors play a crucial role in shaping the overall water quality in the Bagh River
 530 Basin. One important aspect to consider is the computation of the Water Quality Index (WQI),
 531 a comprehensive indicator of water quality. Calculating the WQI can be a complex and time-
 532 consuming due to the numerous parameters and variables involved. Notably, the values of
 533 WQI can vary depending on the specific combination of input parameters used in the
 534 calculation. This variability in results is an essential consideration when interpreting WQI
 535 values, as highlighted in the work of [73].

536 To improve the accuracy of WQI assessments, it's often beneficial to include a wide
 537 range of input parameters in the analysis, as indicated by research findings by Tiwari et al.
 538 [74]. A more comprehensive set of input parameters provides a more holistic view of water
 539 quality, leading to a more realistic representation of the WQI. In contrast, it required more
 540 lab analysis to compute all the water quality parameters, which is time-consuming and costly.
 541 The present study developed and evaluated a new hybrid model (ANN-SVM) to improve the
 542 performance of the ANN model. The results of this investigation have demonstrated that

543 Support Vector Machines (SVM) prove to be a highly effective method for addressing a range
544 of environmental issues, as proven in various studies [75–77].

545 The present study investigated the ANN stand alone and its hybrid five ML models
546 were suitable for predicting WQI (i.e., ANN-RF, ANN-SVM, ANN-RSS, ANN-AR, and ANN-M5P).
547 Based on the Nash-Sutcliffe efficiency (NSE) and root mean squared error (RMSE) in the
548 testing data sets, the order of models' performance for WQI during the testing period was
549 found as ANN-SVM (0.879, 27.974) > ANN (0.842, 31.923) > ANN-M5P (0.782, 37.499) > ANN-
550 RSS (0.742, 40.804) > ANN-AR (0.637, 48.405) > ANN-RF (0.625, 49.224). The results from the
551 machine learning models show that the ANN-SVM model greatly reduces the overall residual
552 errors resulting from the model's accuracy in predicting the future, as shown in the Table 4.
553 The residuals of other machine learning models are larger than those of the ANN-SVM and
554 ANN models, which implies that these other machine learning models are ineffective in
555 accurately estimating the field data due to their larger residuals.

556 The findings of our study align with Nafsin and Li [78] implied the use of a variety of
557 individual machine learning models, including the random forest (RF), artificial neural
558 network (ANN), gradient boosting machine (GBM), support vector machine (SVM), and
559 ensemble-hybrid models such as GBM-SVM, RF-SVM, RF-ANN, ANN-SVM, and RF-GBM for
560 predicting total organic carbon (TOC) and E. coli in the Milwaukee River system. The outcome
561 shows that the ensemble-hybrid model ANN-GBM performed better in forecasting for TOC
562 and E. coli than other models. The effectiveness of six novel hybrid algorithms, including RF-
563 SVM, ANN-SVM, GBM-SVM, RF-ANN, and GBM-ANN, for predicting the BOD of the Buriganga
564 river system in Bangladesh was also examined in a different study. These algorithms included
565 RF-SVM, ANN-SVM, GBM-SVM, RF-ANN, and RF-GBM. One of the study's main findings was
566 the development of a novel hybrid model, the RF-SVM, which has the greatest R^2 value (0.908)
567 and led to higher prediction success. Another study, Singh et al. [79] highlighted the ANN's
568 potential in predicting WQI. Chou et al. [80] compared four ML algorithms for water quality
569 assessment in Taiwanese reservoirs, finding the ANN model to outperform others. Song et al.
570 [81] showed RF's superior prediction accuracy for pressure ulcer modeling compared to SVM,
571 DT, and ANN. Similarly, Castrillo and García [8] favored the RF model over linear regression
572 for nutrient concentration prediction. Lastly, Nafi et al. [24] found RF more accurate than RT
573 for water quality based on precision, accuracy, and recall metrics. The results from the current
574 investigation also found that the ANN and its hybrid model ANN-SVM have a greater

575 predictive capability for water quality indices in the study area. The new hybrid machine
576 learning model that developed can be particularly useful, especially in developing countries,
577 for efficient and methodical data supervision, water pollution control, prediction of
578 hydrological events, and hydro-chemical parameters forecasting and prevention of hazards.
579 However, hybrid AI models have not always been successful in improving the prediction
580 power of standalone models, and in some cases, they were unable to do so either [23]. The
581 present study has not only identified the key drivers of water quality but has also emphasized
582 the importance of considering a broad spectrum of input parameters when calculating the
583 WQI. Adopting modern soft computing techniques also underscores the potential for more
584 efficient and accurate water quality assessments in the Bagh River Basin and similar regions.

585 The suitability of the Bagh River Basin (BRB), a major tributary of the Wainganga River,
586 for irrigation purposes was assessed in this study. We employed the Water Quality Index
587 (WQI) technique to evaluate the quality of irrigation water in the river. The spatial distribution
588 of the WQI map for the Bagh River, generated using GIS, is depicted in Fig. 10. The WQI was
589 categorized into five levels for irrigation purposes: excellent water, good water, poor water,
590 extremely poor water, and unsuitable water. At the Gotobodi and Domatola sampling sites
591 along the Bagh River, a few locations were found to have high WQI levels falling into the
592 "Unsuitable water" category (Fig. 10). It is not advisable to use this water for irrigation.
593 Gotobodi and Domatola recorded the highest WQI values of 376.64 and 369.87, respectively.
594 Generally, as water quality deteriorates, WQI levels increase. The upper reaches of the Bagh
595 River, including areas such as Sukhapur, Ghoti, Mohali, Salegaon, Sakharitola, Gore, Nawatola,
596 Nimba, Zaliya, Paldongri, Bhosa, and Dhudwa, were found to have excellent quality irrigation
597 water. WQI values below 100 indicate that the water is suitable for irrigation in these areas.
598 Good quality irrigation water was observed in the midstream of the Bagh River, particularly
599 in locations like Suryatola, Purgaon, Awa, Kumbhartoli, Pandhari, Kachargarh, Khampura, and
600 Hardoi. However, the water quality was very poor in some areas like Birsi, Thana, Borkanhar,
601 and Murdami villages, as indicated in Fig.10.

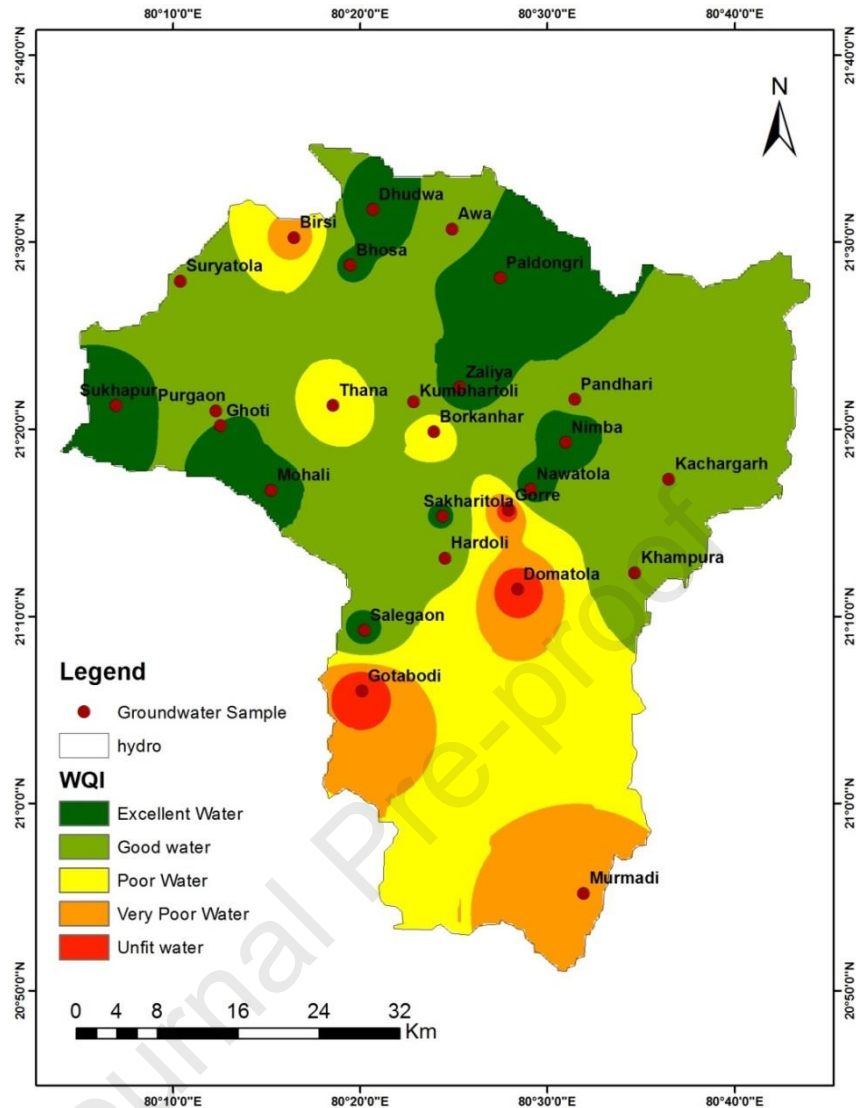


Fig. 10. Spatial distribution of WQI in the study river basin.

602

603

604

605

606

607

608

609

610

611

612

613

The ML algorithms require large datasets for training and testing, but often water quality data are scarce and expensive to obtain. In addition, water quality is affected by various natural and anthropogenic factors, which can make it challenging to collect and interpret data. Therefore, it is important to ensure that the data used to train ML models are accurate, reliable, and representative of the actual water quality conditions. The ML-based WQI prediction has the potential to provide valuable insights into water quality, particularly in areas where traditional monitoring methods are not feasible or cost-intensive. Moreover, ML models can be used to identify the specific factors that are driving water quality degradation, which can help inform targeted and effective management strategies. Therefore, further research is needed to address the practical and technical challenges

614 associated with ML-based WQI prediction and to develop reliable and interpretable models
615 that can be used for decision-making purposes.

616 5. Conclusions

617 The present study proposed a new hybrid model (ANN-SVM) using stacked hybridization
618 to improve the performance of Artificial Neural Networks (ANN) in predicting water quality
619 index (WQI) in the Bagh River Basin, India. The approach developed in the present study uses
620 stacking hybridization to combine various machine learning algorithms. The successful
621 integration of the support vector machine (SVM) with ANN and the use of the Relief algorithm
622 to choose the water quality input parameters that have the greatest influence show improved
623 predictive capabilities with high values of Nash-Sutcliffe efficiency (NSE), Pearson correlation
624 coefficient (PCC), and Coefficient of determination (R²), and low values of Mean absolute
625 error (MAE), Root mean square error (RMSE), Relative root square error (RRSE), Relative
626 absolute error (RAE), and Mean squared Error (MSE). The results obtained were further
627 analyzed and compared using graphical representations to facilitate comprehension. It was
628 observed that, with the exception of SVM, none of the other algorithms demonstrated an
629 enhancement in the performance of ANN. During the validation phase, the model
630 performances were ranked as follows: ANN-SVM (NSE = 0.879) > ANN (NSE = 0.842) > ANN-
631 M5P (NSE = 0.782) > ANN-RSS (NSE = 0.742) > ANN-AR (NSE = 0.637) > ANN-RF (NSE = 0.625).
632 These findings offer significant promise for bolstering informed decision-making in water
633 resource management, pollution control, and environmental conservation efforts.

634 Moreover, the methodology outlined in this study can serve as a valuable framework
635 for refining ANN models across diverse environmental applications, thereby contributing to
636 sustainable development and resource preservation. The present study solely relies on water
637 samples collected within the boundaries of the river basin. Therefore, future research efforts
638 will focus on applying the enhanced AI model across various basins and under diverse climatic
639 conditions to obtain more generalized conclusions.

640 Declaration

641 **Ethics approval:** All authors comply with the guidelines of the journal "*Heliyon*".

642 **Consent to participate:** All authors agreed to participate in this study.

643 **Consent to publication:** All authors agreed to the publication of this manuscript.

644 **Funding:** No funding was received for conducting this study.

645 **Declaration of competing interest**

646 The authors declare that they have no known competing financial interests or personal
647 relationships that could have appeared to influence the work reported in this paper.

648 **Data availability statement**

649 The data pertaining to this study have not been deposited in a publicly accessible repository,
650 given that all relevant data are thoroughly detailed in the article or appropriately cited in the
651 manuscript.

652 **CRediT authorship contribution statement**

653 **N. L. Kushwaha and Nanabhau S. Kudnar:** Conceptualization, Methodology, Formal analysis,
654 Software, Writing- Original draft preparation. **Dinesh Kumar Vishwakarma, Ismail Abd-Elaty,**
655 **and A Subeesh:** Visualization, Comments and Revisions recommendations, Writing-
656 Reviewing and Editing. **N. L. Kushwaha, Nanabhau S. Kudnar, and Dinesh Kumar**
657 **Vishwakarma:** Formal analysis, Software, Validation. **Nanabhau S. Kudnar and Malkhan**
658 **Singh Jatav, Venkatesh Gaddikeri, Ismail Abd-Elaty and Ashraf Ahmed:** Supervision,
659 Comments, and Revisions Recommendations, Writing- Reviewing and Editing.

660 **Acknowledgment**

661 The authors are thankful to the Central Ground Water Board, Central Region (CR), Nagpur,
662 and National Environmental Engineering Research Institute (NEERI), Nagpur, Maharashtra,
663 India, for providing information and support in the present study. Ismail Abd-Elaty thank the
664 Department of Water and Water Structures Engineering, Faculty of Engineering, Zagazig
665 University, Zagazig 44519, Egypt, for constant support during the study.

666 **References**

- 667 [1] Abd-Elaty, Zelenakova, Straface, Vranayová, Abu-hashim, Integrated Modelling for Groundwater
668 Contamination from Polluted Streams Using New Protection Process Techniques, *Water* 11
669 (2019) 2321. <https://doi.org/10.3390/w11112321>.
- 670 [2] I. Abd-Elaty, H. Shoshah, M. Zelenáková, N.L. Kushwaha, O.W. El-Dean, Forecasting of Flash
671 Floods Peak Flow for Environmental Hazards and Water Harvesting in Desert Area of El-Qaa
672 Plain, Sinai, *Int. J. Environ. Res. Public Health* 19 (2022) 6049.
673 <https://doi.org/10.3390/ijerph19106049>.
- 674 [3] N.L. Kushwaha, J. Rajput, T. Suna, D.R. Sena, D.K. Singh, A.K. Mishra, P.K. Sharma, I. Mani,
675 Metaheuristic approaches for prediction of water quality indices with relief algorithm-based
676 feature selection, *Ecol. Inform.* 75 (2023) 102122.
677 <https://doi.org/10.1016/j.ecoinf.2023.102122>.
- 678 [4] G. Guillet, J.L.A. Knapp, S. Merel, O.A. Cirpka, P. Grathwohl, C. Zwiener, M. Schwientek, Fate of
679 wastewater contaminants in rivers: Using conservative-tracer based transfer functions to assess

- 680 reactive transport, *Sci. Total Environ.* 656 (2019) 1250–1260.
 681 <https://doi.org/10.1016/j.scitotenv.2018.11.379>.
- 682 [5] M.G. Zanoni, B. Majone, A. Bellin, A catchment-scale model of river water quality by Machine
 683 Learning, *Sci. Total Environ.* 838 (2022) 156377.
 684 <https://doi.org/10.1016/j.scitotenv.2022.156377>.
- 685 [6] R.P. Schwarzenbach, T. Egli, T.B. Hofstetter, U. von Gunten, B. Wehrli, *Global Water Pollution*
 686 *and Human Health*, *Annu. Rev. Environ. Resour.* 35 (2010) 109–136.
 687 <https://doi.org/10.1146/annurev-environ-100809-125342>.
- 688 [7] E. Diamantini, S.R. Lutz, S. Mallucci, B. Majone, R. Merz, A. Bellin, Driver detection of water
 689 quality trends in three large European river basins, *Sci. Total Environ.* 612 (2018) 49–62.
 690 <https://doi.org/10.1016/j.scitotenv.2017.08.172>.
- 691 [8] M. Castrillo, Á.L. García, Estimation of high frequency nutrient concentrations from water quality
 692 surrogates using machine learning methods, *Water Res.* 172 (2020) 115490.
 693 <https://doi.org/10.1016/j.watres.2020.115490>.
- 694 [9] S. Das, N. Sharma, P. Sharma, N.L. Kushwaha, Assessment of Rainfall (R), Evapotranspiration (ET),
 695 and Crop Coefficient (Kc) Using Satellite Data, in: C.B. Pande, M. Kumar, N.L. Kushwaha (Eds.),
 696 *Surf. Groundw. Resour. Dev. Manag. Semi-Arid Reg. Strateg. Solut. Sustain. Water Manag.*,
 697 Springer International Publishing, Cham, 2023: pp. 365–380. https://doi.org/10.1007/978-3-031-29394-8_19.
- 699 [10] C.B. Pande, M. Kumar, N.L. Kushwaha, eds., *Surface and Groundwater Resources Development*
 700 *and Management in Semi-arid Region: Strategies and Solutions for Sustainable Water*
 701 *Management*, Springer International Publishing, Cham, 2023. <https://doi.org/10.1007/978-3-031-29394-8>.
- 703 [11] G.S. Nearing, F. Kratzert, A.K. Sampson, C.S. Pelissier, D. Klotz, J.M. Frame, C. Prieto, H.V. Gupta,
 704 What Role Does Hydrological Science Play in the Age of Machine Learning?, *Water Resour. Res.*
 705 57 (2021) e2020WR028091. <https://doi.org/10.1029/2020WR028091>.
- 706 [12] C. Shen, A Transdisciplinary Review of Deep Learning Research and Its Relevance for Water
 707 Resources Scientists, *Water Resour. Res.* 54 (2018) 8558–8593.
 708 <https://doi.org/10.1029/2018WR022643>.
- 709 [13] Z.M. Yaseen, S.O. Sulaiman, R.C. Deo, K.-W. Chau, An enhanced extreme learning machine model
 710 for river flow forecasting: State-of-the-art, practical applications in water resource engineering
 711 area and future research direction, *J. Hydrol.* 569 (2019) 387–408.
 712 <https://doi.org/10.1016/j.jhydrol.2018.11.069>.
- 713 [14] D.P. Nguyen, H.D. Ha, N.T. Trinh, M.T. Nguyen, Application of artificial intelligence for forecasting
 714 surface quality index of irrigation systems in the Red River Delta, Vietnam, *Environ. Syst. Res.* 12
 715 (2023) 24. <https://doi.org/10.1186/s40068-023-00307-6>.
- 716 [15] A. Patel, A. Kethavath, N.L. Kushwaha, A. Naorem, M. Jagadale, S. K.r., R. P.s., Review of artificial
 717 intelligence and internet of things technologies in land and water management research during
 718 1991–2021: A bibliometric analysis, *Eng. Appl. Artif. Intell.* 123 (2023) 106335.
 719 <https://doi.org/10.1016/j.engappai.2023.106335>.
- 720 [16] R.K. Horton, An index number system for rating water quality, *J. Water Pollut. Control Fed.* 37
 721 (1965) 300–306.
- 722 [17] V.M. Wagh, D.B. Panaskar, A.A. Muley, S.V. Mukate, Y.P. Lolage, M.L. Aamalawar, Prediction of
 723 groundwater suitability for irrigation using artificial neural network model: a case study of
 724 Nanded tehsil, Maharashtra, India, *Model. Earth Syst. Environ.* 2 (2016) 1–10.
 725 <https://doi.org/10.1007/s40808-016-0250-3>.
- 726 [18] J.C. Egbueri, J.C. Agbasi, Combining data-intelligent algorithms for the assessment and predictive
 727 modeling of groundwater resources quality in parts of southeastern Nigeria, *Environ. Sci. Pollut.*
 728 *Res.* 29 (2022) 57147–57171. <https://doi.org/10.1007/s11356-022-19818-3>.
- 729 [19] R. Massei, W. Busch, H. Wolschke, L. Schinkel, M. Bitsch, T. Schulze, M. Krauss, W. Brack,
 730 Screening of Pesticide and Biocide Patterns As Risk Drivers in Sediments of Major European River

- 731 Mouths: Ubiquitous or River Basin-Specific Contamination?, *Environ. Sci. Technol.* 52 (2018)
 732 2251–2260. <https://doi.org/10.1021/acs.est.7b04355>.
- 733 [20] S. Shamshirband, E. Jafari Nodoushan, J.E. Adolf, A. Abdul Manaf, A. Mosavi, K. Chau, Ensemble
 734 models with uncertainty analysis for multi-day ahead forecasting of chlorophyll a concentration
 735 in coastal waters, *Eng. Appl. Comput. Fluid Mech.* 13 (2019) 91–101.
 736 <https://doi.org/10.1080/19942060.2018.1553742>.
- 737 [21] Z. Di, M. Chang, P. Guo, Water Quality Evaluation of the Yangtze River in China Using Machine
 738 Learning Techniques and Data Monitoring on Different Time Scales, *Water* 11 (2019) 339.
 739 <https://doi.org/10.3390/w11020339>.
- 740 [22] Ahmed AA, Sayed S, Abdoulhalik A, Moutari S, Oyedele L. Applications of machine learning to
 741 water resources management: A review of present status and future opportunities. *Journal of*
 742 *Cleaner Production.* 2024 Jan 11:140715.
- 743 [23] D.T. Bui, K. Khosravi, J. Tiefenbacher, H. Nguyen, N. Kazakis, Improving prediction of water
 744 quality indices using novel hybrid machine-learning algorithms, *Sci. Total Environ.* 721 (2020)
 745 137612. <https://doi.org/10.1016/j.scitotenv.2020.137612>.
- 746 [24] S.N.M.M. Nafi, A. Mustapha, S.A. Mostafa, S.H. Khaleefah, M.N. Razali, Experimenting Two
 747 Machine Learning Methods in Classifying River Water Quality, in: M.I. Khalaf, D. Al-Jumeily, A.
 748 Lisitsa (Eds.), *Appl. Comput. Support Ind. Innov. Technol.*, Springer International Publishing,
 749 Cham, 2020: pp. 213–222. https://doi.org/10.1007/978-3-030-38752-5_17.
- 750 [25] J.C. Agbasi, J.C. Egbueri, Assessment of PTEs in water resources by integrating HHRISK code,
 751 water quality indices, multivariate statistics, and ANNs, *Geocarto Int.* 37 (2022) 10407–10433.
 752 <https://doi.org/10.1080/10106049.2022.2034990>.
- 753 [26] H.S. Jahin, A.S. Abuzaid, A.D. Abdellatif, Using multivariate analysis to develop irrigation water
 754 quality index for surface water in Kafr El-Sheikh Governorate, Egypt, *Environ. Technol. Innov.* 17
 755 (2020) 100532. <https://doi.org/10.1016/j.eti.2019.100532>.
- 756 [27] A. Elbeltagi, C.B. Pande, S. Kouadri, A.R.Md.T. Islam, Applications of various data-driven models
 757 for the prediction of groundwater quality index in the Akot basin, Maharashtra, India, *Environ.*
 758 *Sci. Pollut. Res.* 29 (2022) 17591–17605. <https://doi.org/10.1007/s11356-021-17064-7>.
- 759 [28] S. Kouadri, A. Elbeltagi, A.R.Md.T. Islam, S. Kateb, Performance of machine learning methods in
 760 predicting water quality index based on irregular data set: application on Illizi region (Algerian
 761 southeast), *Appl. Water Sci.* 11 (2021) 190. <https://doi.org/10.1007/s13201-021-01528-9>.
- 762 [29] M. Valentini, G.B. dos Santos, B. Muller Vieira, Multiple linear regression analysis (MLR) applied
 763 for modeling a new WQI equation for monitoring the water quality of Mirim Lagoon, in the state
 764 of Rio Grande do Sul—Brazil, *SN Appl. Sci.* 3 (2021) 70. <https://doi.org/10.1007/s42452-020-04005-1>.
- 766 [30] V.K. Gautam, C.B. Pande, K.N. Moharir, A.M. Varade, N.L. Rane, J.C. Egbueri, F. Alshehri,
 767 Prediction of Sodium Hazard of Irrigation Purpose using Artificial Neural Network Modelling,
 768 *Sustainability* 15 (2023) 7593. <https://doi.org/10.3390/su15097593>.
- 769 [31] R. Shukla, P. Kumar, D.K. Vishwakarma, R. Ali, R. Kumar, A. Kuriqi, Modeling of stage-discharge
 770 using back propagation ANN-, ANFIS-, and WANN-based computing techniques, *Theor. Appl.*
 771 *Climatol.* 147 (2022) 867–889. <https://doi.org/10.1007/s00704-021-03863-y>.
- 772 [32] N.S. Kudnar, GIS-based assessment of morphological and hydrological parameters of Wainganga
 773 River Basin, Central India, *Model. Earth Syst. Environ.* 6 (2020) 1933–1950.
 774 <https://doi.org/10.1007/s40808-020-00804-y>.
- 775 [33] N.S. Kudnar, V.N. Mishra, M. Rajashekhar, Hydro-Chemical Characterization and Geospatial
 776 Analysis of Groundwater for Drinking and Agriculture Usage in Bagh River Basin, Central India,
 777 in: P.K. Rai (Ed.), *River Conserv. Water Resour. Manag.*, Springer Nature, Singapore, 2023: pp.
 778 95–116. https://doi.org/10.1007/978-981-99-2605-3_6.

- 779 [34] P.R. Shekar, A. Mathew, Evaluation of Morphometric and Hypsometric Analysis of the Bagh River
780 Basin using Remote Sensing and Geographic Information System Techniques, *Energy Nexus* 7
781 (2022) 100104. <https://doi.org/10.1016/j.nexus.2022.100104>.
- 782 [35] N. Akhtar, M.I.S. Ishak, M.I. Ahmad, K. Umar, M.S. Md Yusuff, M.T. Anees, A. Qadir, Y.K. Ali
783 Almanasir, Modification of the Water Quality Index (WQI) Process for Simple Calculation Using
784 the Multi-Criteria Decision-Making (MCDM) Method: A Review, *Water* 13 (2021) 905.
785 <https://doi.org/10.3390/w13070905>.
- 786 [36] M.G. Uddin, S. Nash, A. Rahman, A.I. Olbert, A comprehensive method for improvement of water
787 quality index (WQI) models for coastal water quality assessment, *Water Res.* 219 (2022) 118532.
788 <https://doi.org/10.1016/j.watres.2022.118532>.
- 789 [37] WHO, Guidelines for Drinking-water Quality- 4th ed., World Health Organization, Geneva, 2011.
790 [https://apps.who.int/iris/bitstream/handle/10665/44584/9789241548151_eng.pdf;jsessionid=](https://apps.who.int/iris/bitstream/handle/10665/44584/9789241548151_eng.pdf;jsessionid=6A5AE9F7BBF06EF78B1C62856FCA9638?sequence=1)
791 [6A5AE9F7BBF06EF78B1C62856FCA9638?sequence=1](https://apps.who.int/iris/bitstream/handle/10665/44584/9789241548151_eng.pdf;jsessionid=6A5AE9F7BBF06EF78B1C62856FCA9638?sequence=1).
- 792 [38] I.A. Basheer, M. Hajmeer, Artificial neural networks: fundamentals, computing, design, and
793 application, *J. Microbiol. Methods* 43 (2000) 3–31. [https://doi.org/10.1016/S0167-](https://doi.org/10.1016/S0167-7012(00)00201-3)
794 [7012\(00\)00201-3](https://doi.org/10.1016/S0167-7012(00)00201-3).
- 795 [39] R.J. Schalkoff, Artificial neural networks, McGraw-Hill Higher Education, 1997.
- 796 [40] A. Subeesh, C.R. Mehta, Automation and digitization of agriculture using artificial intelligence
797 and internet of things, *Artif. Intell. Agric.* 5 (2021) 278–291.
798 <https://doi.org/10.1016/j.iaia.2021.11.004>.
- 799 [41] A. Malekian, N. Chitsaz, Chapter 4 - Concepts, procedures, and applications of artificial neural
800 network models in streamflow forecasting, in: P. Sharma, D. Machiwal (Eds.), *Adv. Streamflow*
801 *Forecast.*, Elsevier, 2021: pp. 115–147. <https://doi.org/10.1016/B978-0-12-820673-7.00003-2>.
- 802 [42] R. Sadiq, M.J. Rodriguez, H.R. Mian, Empirical models to predict disinfection by-products (DBPs)
803 in drinking water: An updated review, (2019).
- 804 [43] T.K. Ho, The random subspace method for constructing decision forests, *IEEE Trans. Pattern Anal.*
805 *Mach. Intell.* 20 (1998) 832–844. <https://doi.org/10.1109/34.709601>.
- 806 [44] C. Sammut, G.I. Webb, eds., Random Subspace Method, in: *Encycl. Mach. Learn. Data Min.*,
807 Springer US, Boston, MA, 2017: pp. 1055–1055. [https://doi.org/10.1007/978-1-4899-7687-](https://doi.org/10.1007/978-1-4899-7687-1_696)
808 [1_696](https://doi.org/10.1007/978-1-4899-7687-1_696).
- 809 [45] L.I. Kuncheva, J.J. Rodriguez, C.O. Plumpton, D.E.J. Linden, S.J. Johnston, Random Subspace
810 Ensembles for fMRI Classification, *IEEE Trans. Med. Imaging* 29 (2010) 531–542.
811 <https://doi.org/10.1109/TMI.2009.2037756>.
- 812 [46] N.L. Kushwaha, J. Rajput, A. Elbeltagi, A.Y. Elnaggar, D.R. Sena, D.K. Vishwakarma, I. Mani, E.E.
813 Hussein, Data Intelligence Model and Meta-Heuristic Algorithms-Based Pan Evaporation
814 Modelling in Two Different Agro-Climatic Zones: A Case Study from Northern India, *Atmosphere*
815 12 (2021) 1654. <https://doi.org/10.3390/atmos12121654>.
- 816 [47] R.G. Brereton, G.R. Lloyd, Support Vector Machines for classification and regression, *Analyst* 135
817 (2010) 230–267. <https://doi.org/10.1039/B918972F>.
- 818 [48] A. Shmilovici, Support vector machines, in: *Data Min. Knowl. Discov. Handb.*, Springer, 2009: pp.
819 231–247.
- 820 [49] M. Stitson, J. Weston, A. Gammerman, V. Vovk, V. Vapnik, Theory of support vector machines,
821 *Univ. Lond.* 117 (1996) 188–191.
- 822 [50] M. Awad, R. Khanna, Support Vector Regression, in: M. Awad, R. Khanna (Eds.), *Effic. Learn.*
823 *Mach. Theor. Concepts Appl. Eng. Syst. Des.*, Apress, Berkeley, CA, 2015: pp. 67–80.
824 https://doi.org/10.1007/978-1-4302-5990-9_4.
- 825 [51] M. Mohammady, H.R. Pourghasemi, M. Amiri, Land subsidence susceptibility assessment using
826 random forest machine learning algorithm, *Environ. Earth Sci.* 78 (2019) 1–12.
827 <https://doi.org/10.1007/s12665-019-8518-3>.
- 828 [52] M.R. Segal, Machine Learning Benchmarks and Random Forest Regression, (2004).
829 <https://escholarship.org/uc/item/35x3v9t4> (accessed December 24, 2022).

- 830 [53] G. Biau, E. Scornet, A random forest guided tour, *TEST* 25 (2016) 197–227.
831 <https://doi.org/10.1007/s11749-016-0481-7>.
- 832 [54] S. Misra, H. Li, Chapter 9 - Noninvasive fracture characterization based on the classification of
833 sonic wave travel times, in: S. Misra, H. Li, J. He (Eds.), *Mach. Learn. Subsurf. Charact.*, Gulf
834 Professional Publishing, 2020: pp. 243–287. <https://doi.org/10.1016/B978-0-12-817736-5.00009-0>.
- 835
836 [55] J.H. Friedman, Stochastic gradient boosting, *Comput. Stat. Data Anal.* 38 (2002) 367–378.
837 [https://doi.org/10.1016/S0167-9473\(01\)00065-2](https://doi.org/10.1016/S0167-9473(01)00065-2).
- 838 [56] M.O. Elish, Improved estimation of software project effort using multiple additive regression
839 trees, *Expert Syst. Appl.* 36 (2009) 10774–10778. <https://doi.org/10.1016/j.eswa.2009.02.013>.
- 840 [57] J.R. Quinlan, Learning With Continuous Classes, in: 5th Aust. Jt. Conf. Artif. Intell., World
841 Scientific, 1992: pp. 343–348.
- 842 [58] P. Sihag, S. Mohsenzadeh Karimi, A. Angelaki, Random forest, MSP and regression analysis to
843 estimate the field unsaturated hydraulic conductivity, *Appl. Water Sci.* 9 (2019) 129.
844 <https://doi.org/10.1007/s13201-019-1007-8>.
- 845 [59] B. Singh, P. Sihag, K. Singh, Modelling of impact of water quality on infiltration rate of soil by
846 random forest regression, *Model. Earth Syst. Environ.* 3 (2017) 999–1004.
847 <https://doi.org/10.1007/s40808-017-0347-3>.
- 848 [60] K. Kira, L.A. Rendell, A Practical Approach to Feature Selection, in: D. Sleeman, P. Edwards (Eds.),
849 *Mach. Learn. Proc. 1992*, Morgan Kaufmann, San Francisco (CA), 1992: pp. 249–256.
850 <https://doi.org/10.1016/B978-1-55860-247-2.50037-1>.
- 851 [61] R.J. Urbanowicz, M. Meeker, W. La Cava, R.S. Olson, J.H. Moore, Relief-Based Feature Selection:
852 Introduction and Review, *J. Biomed. Inform.* 85 (2018) 189–203.
853 <https://doi.org/10.1016/j.jbi.2018.07.014>.
- 854 [62] Y. Dagli, Feature selection using Relief algorithms with python example., *Medium* (2019).
855 [https://medium.com/@yashdagli98/feature-selection-using-relief-algorithms-with-python-](https://medium.com/@yashdagli98/feature-selection-using-relief-algorithms-with-python-example-3c2006e18f83)
856 [example-3c2006e18f83](https://medium.com/@yashdagli98/feature-selection-using-relief-algorithms-with-python-example-3c2006e18f83) (accessed August 10, 2023).
- 857 [63] D.H. Wolpert, Stacked generalization, *Neural Netw.* 5 (1992) 241–259.
858 [https://doi.org/10.1016/S0893-6080\(05\)80023-1](https://doi.org/10.1016/S0893-6080(05)80023-1).
- 859 [64] S.P. Healey, W.B. Cohen, Z. Yang, C. Kenneth Brewer, E.B. Brooks, N. Gorelick, A.J. Hernandez, C.
860 Huang, M. Joseph Hughes, R.E. Kennedy, T.R. Loveland, G.G. Moisen, T.A. Schroeder, S.V.
861 Stehman, J.E. Vogelmann, C.E. Woodcock, L. Yang, Z. Zhu, Mapping forest change using stacked
862 generalization: An ensemble approach, *Remote Sens. Environ.* 204 (2018) 717–728.
863 <https://doi.org/10.1016/j.rse.2017.09.029>.
- 864 [65] M. Rahman, N. Chen, A. Elbeltagi, M.M. Islam, M. Alam, H.R. Pourghasemi, W. Tao, J. Zhang, T.
865 Shufeng, H. Faiz, M.A. Baig, A. Dewan, Application of stacking hybrid machine learning
866 algorithms in delineating multi-type flooding in Bangladesh, *J. Environ. Manage.* 295 (2021)
867 113086. <https://doi.org/10.1016/j.jenvman.2021.113086>.
- 868 [66] A. Elbeltagi, F. Di Nunno, N.L. Kushwaha, G. de Marinis, F. Granata, River flow rate prediction in
869 the Des Moines watershed (Iowa, USA): a machine learning approach, *Stoch. Environ. Res. Risk*
870 *Assess.* (2022). <https://doi.org/10.1007/s00477-022-02228-9>.
- 871 [67] N.L. Kushwaha, J. Rajput, D.R. Sena, A. Elbeltagi, D.K. Singh, I. Mani, Evaluation of Data-driven
872 Hybrid Machine Learning Algorithms for Modelling Daily Reference Evapotranspiration,
873 *Atmosphere-Ocean* 60 (2022) 519–540. <https://doi.org/10.1080/07055900.2022.2087589>.
- 874 [68] C.B. Pande, N.L. Kushwaha, I.R. Orimoloye, R. Kumar, H.G. Abdo, A.D. Tolche, A. Elbeltagi,
875 Comparative Assessment of Improved SVM Method under Different Kernel Functions for
876 Predicting Multi-scale Drought Index, *Water Resour. Manag.* 37 (2023) 1367–1399.
877 <https://doi.org/10.1007/s11269-023-03440-0>.
- 878 [69] D.K. Vishwakarma, K. Pandey, A. Kaur, N.L. Kushwaha, R. Kumar, R. Ali, A. Elbeltagi, A. Kuriqi,
879 Methods to estimate evapotranspiration in humid and subtropical climate conditions, *Agric.*
880 *Water Manag.* 261 (2022) 107378. <https://doi.org/10.1016/j.agwat.2021.107378>.

- 881 [70] S. Markuna, P. Kumar, R. Ali, D.K. Vishwkarma, K.S. Kushwaha, R. Kumar, V.K. Singh, S.
882 Chaudhary, A. Kuriqi, Application of Innovative Machine Learning Techniques for Long-Term
883 Rainfall Prediction, *Pure Appl. Geophys.* 180 (2023) 335–363. [https://doi.org/10.1007/s00024-](https://doi.org/10.1007/s00024-022-03189-4)
884 022-03189-4.
- 885 [71] K.E. Taylor, Summarizing multiple aspects of model performance in a single diagram, *J. Geophys.*
886 *Res. Atmospheres* 106 (2001) 7183–7192. <https://doi.org/10.1029/2000JD900719>.
- 887 [72] D.K. Vishwakarma, A. Kuriqi, S.A. Abed, G. Kishore, N. Al-Ansari, K. Pandey, P. Kumar, N.L.
888 Kushwaha, A. Jewel, Forecasting of stage-discharge in a non-perennial river using machine
889 learning with gamma test, *Heliyon* 9 (2023). <https://doi.org/10.1016/j.heliyon.2023.e16290>.
- 890 [73] Tiyasha, T.M. Tung, Z.M. Yaseen, A survey on river water quality modelling using artificial
891 intelligence models: 2000–2020, *J. Hydrol.* 585 (2020) 124670.
892 <https://doi.org/10.1016/j.jhydrol.2020.124670>.
- 893 [74] S. Tiwari, R. Babbar, G. Kaur, Performance Evaluation of Two ANFIS Models for Predicting Water
894 Quality Index of River Satluj (India), *Adv. Civ. Eng.* 2018 (2018) 1–10.
895 <https://doi.org/10.1155/2018/8971079>.
- 896 [75] D. Dimple, J. Rajput, N. Al-Ansari, A. Elbeltagi, Predicting Irrigation Water Quality Indices Based
897 on Data-Driven Algorithms: Case Study in Semiarid Environment, *J. Chem.* 2022 (2022)
898 e4488446. <https://doi.org/10.1155/2022/4488446>.
- 899 [76] M. Koranga, P. Pant, D. Pant, A.K. Bhatt, R.P. Pant, M. Ram, T. Kumar, SVM Model to Predict the
900 Water Quality Based on Physicochemical Parameters, *Int. J. Math. Eng. Manag. Sci.* 6 (2021) 645–
901 659. <https://doi.org/10.33889/IJMEMS.2021.6.2.040>.
- 902 [77] M. Najafzadeh, S. Niazmardi, A Novel Multiple-Kernel Support Vector Regression Algorithm for
903 Estimation of Water Quality Parameters, *Nat. Resour. Res.* 30 (2021) 3761–3775.
904 <https://doi.org/10.1007/s11053-021-09895-5>.
- 905 [78] N. Nafsin, J. Li, Prediction of total organic carbon and E. coli in rivers within the Milwaukee River
906 basin using machine learning methods, *Environ. Sci. Adv.* 2 (2023) 278–293.
907 <https://doi.org/10.1039/D2VA00285J>.
- 908 [79] S. Singha, S. Pasupuleti, S.S. Singha, R. Singh, S. Kumar, Prediction of groundwater quality using
909 efficient machine learning technique, *Chemosphere* 276 (2021) 130265.
910 <https://doi.org/10.1016/j.chemosphere.2021.130265>.
- 911 [80] J.-S. Chou, C.-C. Ho, H.-S. Hoang, Determining quality of water in reservoir using machine
912 learning, *Ecol. Inform.* 44 (2018) 57–75. <https://doi.org/10.1016/j.ecoinf.2018.01.005>.
- 913 [81] J. Song, Y. Gao, P. Yin, Y. Li, Y. Li, J. Zhang, Q. Su, X. Fu, H. Pi, The Random Forest Model Has the
914 Best Accuracy Among the Four Pressure Ulcer Prediction Models Using Machine Learning
915 Algorithms, *Risk Manag. Healthc. Policy* 14 (2021) 1175–1187.
916 <https://doi.org/10.2147/RMHP.S297838>.
- 917

Highlights

- A comparative study of ANN and its hybrid models (i.e., ANN-RF, ANN-SVM, ANN-RSS, ANN-AR, and ANN-M5P) was conducted for water quality assessment.
- Integrating SVM with ANN significantly improved the model performance.
- The new model can serve as a template for various environmental applications.
- This advancement holds promising decisions in water resource management.

Journal Pre-proof

Declaration of interests

The authors declare that they have no known competing financial interests or personal relationships that could have appeared to influence the work reported in this paper.

The authors declare the following financial interests/personal relationships which may be considered as potential competing interests:

Journal Pre-proof